Integrative Biology

Dynamic Article Links

Cite this: *Integr. Biol.*, 2011, **3**, 603–631

www.rsc.org/ibiology

REVIEW ARTICLE

The challenges of integrating molecular imaging into the optimization of cancer therapy

G. S. Patel,*[ab] T. Kiuchi,[ac] K. Lawler,[d] E. Ofo,[ae] G. O. Fruhwirth,[a] M. Kelleher,[af] E. Shamil,[a] R. Zhang,[g] P. R. Selvin,[g] G. Santis,[h] J. Spicer,[b] N. Woodman,[i] C. E. Gillett,[ci] P. R. Barber,[j] B. Vojnovic,[jk] G. Kéri,[lm] T. Schaeffter,[n] V. Goh,[n] M. J. O'Doherty,[o] P. A. Ellis[b] and T. Ng*[ac]

Received 23rd October 2010, Accepted 2nd March 2011
DOI: 10.1039/c0ib00131g

We review novel, *in vivo* and tissue-based imaging technologies that monitor and optimize cancer therapeutics. Recent advances in cancer treatment centre around the development of targeted therapies and personalisation of treatment regimes to individual tumour characteristics. However, clinical outcomes have not improved as expected. Further development of the use of molecular imaging to predict or assess treatment response must address spatial heterogeneity of cancer within the body. A combination of different imaging modalities should be used to relate the effect of the drug to dosing regimen or effective drug concentration at the local site of action. Molecular imaging provides a functional and dynamic read-out of cancer therapeutics, from nanometre to whole body scale. At the whole body scale, an increase in the sensitivity and specificity of the imaging probe is required to localise (micro)metastatic foci and/or residual disease that are currently below the limit of detection. The use of image-guided endoscopic biopsy can produce tumour cells or tissues for nanoscopic analysis in a relatively patient-compliant manner, thereby linking clinical imaging to a more precise assessment of molecular mechanisms.
This multimodality imaging approach (in combination with genetics/genomic information) could be used to bridge the gap between our knowledge of mechanisms underlying the processes of metastasis, tumour dormancy and routine clinical practice. Treatment regimes could therefore be individually tailored both at diagnosis and throughout treatment, through monitoring of drug pharmacodynamics providing an early read-out of response or resistance.

1. Introduction

Cancer therapies have evolved significantly over the past ten years with the advent of targeted treatments designed to a specific pathogenic process. Since the widespread adoption of the human epidermal growth factor (HER) inhibitor, trastuzumab (a monoclonal antibody to the extracellular domain of HER2) for HER2 overexpressing breast cancer,

[a] *Richard Dimbleby Department of Cancer Research, Randall Division & Division of Cancer Studies, King's College London, Guy's Medical School Campus, London, SE1 1UL, UK. E-mail: gargi.patel@kcl.ac.uk, tony.ng@kcl.ac.uk; Tel: +44(0) 20 7848 6174*
[b] *Research Oncology, Division of Cancer Studies, King's College London, Guy's Campus, London, SE1 9RT, UK*
[c] *Breakthrough Breast Cancer Research Unit, Research Oncology, King's College London, Guy's Medical School Campus, London, SE1 9RT, UK*
[d] *Comprehensive Cancer Imaging Centre, King's College London, New Hunt's House, Guy's Medical School Campus, London, SE1 1UL, UK*
[e] *Department of Otolaryngology Head & Neck Surgery, Guy's & St Thomas' NHS Foundation Trust, London, SE1 1UL, UK*
[f] *Department of Medical Oncology, St. George's Hospital, London, SW17 0QT, UK*
[g] *Center for Biophysics and Computational Biology, Department of Physics, and the Center of Physics of Living Cells, University of Illinois, Urbana-Champaign, USA*
[h] *Department of Asthma Allergy & Respiratory Science, King's College London, Guy's Hospital, London, SE1 9RT, UK*
[i] *Guy's & St Thomas' Breast Tissue & Data Bank, King's College London, Guy's Hospital, London, SE1 9RT, UK*
[j] *Gray Institute for Radiation Oncology & Biology, University of Oxford, Old Road Campus Research Building, Roosevelt Drive, Oxford, OX3 7DQ, UK*
[k] *Randall Division of Cell & Molecular Biophysics, King's College London, London, UK*
[l] *Vichem Chemie Research Ltd., Herman Ottó utca 15, Budapest, Hungary*
[m] *Semmelweis University, Pathobiochemistry Research Group of Hungarian Academy of Science, 1444. Bp 8. POB 260 Hungary*
[n] *Division of Imaging Sciences, King's College London, London, SE1 7EH, UK*
[o] *PET Imaging Centre at St Thomas' Hospital, Division of Imaging Sciences, King's College London, London, SE1 7EH, UK*

there has been a surge in the development of targeted, potential anti-cancer drugs. During drug development, only one in 10 000 compounds screened at the target localization stage will gain approval for clinical use. This process may take more than 10 years.[1] Furthermore, once the drug is within the clinical sphere, clinical outcomes rarely meet initial expectations.

As an example, single-agent phase II studies of epidermal growth factor receptor (EGFR/HER1) inhibitors have shown response rates only of the order of 5–15% in non-small cell lung cancer (NSCLC), head and neck squamous cell carcinoma (HNSCC), and colorectal cancer.[2] The tyrosine kinase inhibitors (TKI), erlotinib and gefitinib, are targeted to EGFR, and approved for use in non-small cell lung cancer.[3] However, response rates are less than 10% in unselected populations and overexpression of EGFR does not correlate with response to treatment.[4] Investigation of somatic gain-of-function mutations in EGFR, led to the discovery of a missense mutation L858R in the EGFR activation loop which facilitates gefitinib binding.[5] This and other activating mutations are correlated with a much improved response rate to TKI therapy, and have helped revolutionise the treatment regimens for NSCLC patients. However, further mutations conferring resistance (especially T790M) can occur which render EGFR resistant to first generation inhibitors.[6] Multiple mutations that confer resistance to the BCR-ABL tyrosine kinase inhibitor imatinib also exist in patients with chronic myelogenous leukaemia (CML).[7] In these CML patients, the genetic basis of additional molecular changes that occur and give rise to secondary drug resistance is frequently unknown. **Thus understanding the molecular genotype does not provide the complete explanation for resistance to molecule-targeted therapies**.

Here we propose that by combining different modalities of molecular imaging we can begin to delineate and quantify the specific molecular pathway alterations within the cancer patient at a subcellular level. The cancer genome or proteome is relatively plastic and can be reprogrammed, at different stages of tumour development, to carry out various cellular processes such as proliferation, invasion and metastasis, or reversion to dormancy.[8] This plasticity gives rise to spatial heterogeneity of cancer within the body and makes it challenging to fully assess treatment response. Molecular imaging provides a solution by mapping the spatial response of the tumour to treatment within the individual and thereby, to monitor progress throughout the patient journey.

For instance, translational research may identify novel biomarkers in the malignant phenotype, which can be imaged by radioligands or tracers, designed specifically to target molecules intrinsic to oncogenesis. Examples of imaging biomarkers include tracers specific to hypoxia, angiogenesis, apoptosis and proliferation.[9] Although novel imaging biomarkers may provide a non-invasive functional read-out of the malignant genome or proteome throughout treatment, there are many challenges in the integration of these biomarkers into clinical practice.

2. Overview of challenges in the implementation of molecular imaging for improving therapeutic efficacy

Molecular imaging may provide an assessment of the temporal and spatial distribution of a probe or biomarker within a disease process. However the main challenge is to find the 'ideal' imaging biomarker which should possess several characteristics, in order to accurately assess the effect of a therapeutic intervention and fulfil clinical utility. These are summarised in Box 1 below.[10] Several key areas are further discussed in the subsequent subsections (2.1–2.4). In particular, in terms of clinical imaging, the second point regarding the activation state of a specific molecular target, which often may be concentration-independent, is seldom addressed in the literature. For this reason we have devoted a whole section (5) in this review to this topic.

Box 1. Ideal features of a molecular imaging biomarker

- Ability to detect specific changes at the molecular (in terms of concentration) level
- Detection of the activated state of molecular target (which is independent of concentration), *e.g.* ligand bound or receptor dimerisation, as a read-out for monitoring drug efficacy
- Safe for human use
- High sensitivity and specificity to distinguish target from background or confounding signals *e.g.* slow tumour washout compared to normal tissue to maintain good signal-to-noise ratio
- Detection of established 'on target' drug effects *in vivo* to assess drug efficacy and response

† Micrometastases were originally defined as small occult metastases of less than 0.2 cm in diameter. Nowadays, the term refers to the spread of cancer cells in groups that are still so small they can only be seen under a microscope, and includes disseminated tumour cells that are present in peripheral blood, bone marrow or lymph nodes.

Insight, innovation, integration

We review novel, *in vivo* and tissue-based imaging technologies that monitor and optimize cancer therapeutics. Clinical outcomes have lagged behind development of targeted therapies. Combinations of imaging modalities should be used to assess tumour spatial heterogeneity, treatment response, and relate drug effects to dosing schedule.

Molecular imaging provides a functional and dynamic read-out of therapeutic response, from nanometre to whole body scale. An increase in imaging probe sensitivity and specificity is required to localise (micro) metastatic† foci that are currently below systemic detection limits.

Image-guided biopsy is key in the multimodality imaging approach needed to bridge the gap between mechanisms underlying pathological processes and clinical practice. Description of novel pharmacodynamic endpoints using this approach can provide early read-out of response or resistance.

(*continued*)

Box 1. Ideal features of a molecular imaging biomarker

- Appropriate 'off-rate' or dissociation constant for adequate imaging but allows washout of biomarker prior to the next assessment.
- Rapid plasma clearance
- Low hepatic excretion to visualise liver metastases
- Rapid, simple chemical synthesis for tracer manufacture
- Inexpensive

2.1 Sensitivity and specificity issues

A difficult balance must be achieved whereby the tracer has a high affinity for the target, which may be present in very small amounts, but low affinity for normal tissue to eliminate background noise. For example, somatostatin analogues have been in use for several decades to image gastroenteropancreatic tumours, as they have a high affinity for the somatostatin receptor (SSR)-2 which is overexpressed by these tumours and in the central nervous system.[11] Somatostatin is the ligand for SSRs but has a short half-life, which limits its use as an imaging agent. Somatostatin analogues are more stable, yet bind as the native ligand, thus conferring high specificity and sensitivity to this imaging modality. The PET analogues [^{68}Ga-DOTA, Tyr3]-octreotide or [^{68}Ga-DOTA, Tyr3]octreotate are emerging as the new standard.[12] These analogues can be labelled with ^{90}Y or ^{177}Lu for use as radionuclide therapy with success as a palliative treatment, thus translating imaging to therapeutics in a single step.[13,14]

The capacity of a biomarker to identify specific cells within the tumour population may describe tumour characteristics,

G. S. Patel

Gargi Patel, a medical oncologist, completed her undergraduate medical degree at the University of Cambridge with a distinction. She carried out her junior doctor training at Guys and St. Thomas Hospital, amongst other London teaching university hospitals. She interrupted her specialist training in order to carry out a PhD at Kings College London, using FRET/FLIM assays in breast cancer, under Prof Tony Ng. She is in her second year, and recently received the McElwain Fellowship from Cancer Research UK for her research.

T. Kiuchi

Tai Kiuchi, a biophysicist, completed his PhD degree in the Biophysical Laboratory (Prof. Kazuo Ohki) at the Department of Physics, Tohoku University, Japan. He has worked for four years as a postdoctoral fellow in the Molecular Biological Laboratory (Prof. Kensaku Mizuno) at the Department of Life Sciences, Tohoku University. He was trained in microscopic imaging techniques and molecular, biological and biochemical techniques. Currently he is researching EGFR ubiquitination and signalling downstream of homo and heterodimers of the HER family using FRET/FLIM assays and molecular biological experiments.

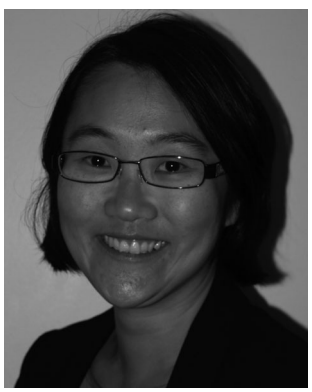

V. Goh

Vicky Goh, Professor of Clinical Cancer Imaging, King's College London and Honorary Consultant Radiologist, Guys and St Thomas' NHS Foundation Trust, graduated with a First from University of Cambridge, underwent her training in medicine and radiology in London, a Fellowship in cross-sectional imaging in Toronto, and was a Consultant Radiologist at Mount Vernon Hospital, Northwood prior to her Chair. Her research programme focuses on the clinical imaging of the tumour microenvironment (vascularity, hypoxia, and water diffusion) and tumour heterogeneity with CT, MRI (including DCE-MRI, BOLD-MRI, and DW-MRI) and PET–CT with particular reference to gastrointestinal, renal and lung cancers.

M. J. O'Doherty

Michael O'Doherty, a nuclear medicine physician, with a special interest in clinical applications of PET–CT. Professor of PET and Nuclear Medicine in Imaging Sciences at Kings College London and Guy's and St Thomas' NHS Foundation Trust.

such as resistance to treatment. For instance, CD133+/CXCR4+ tumour-initiator cells have been shown to undergo a 2-fold increase as a subpopulation (from 3.5% to 7.5% of tumour cells) following *in vivo* cisplatin treatment of lung tumour xenografts in mice, as an indication of the intrinsic resistance of this cell population to chemotherapy.[15] While molecular imaging of CXCR4 in a murine model of breast cancer metastasis with [^{64}Cu]AMD3100 has recently been published,[16] it is likely that its ultimate clinical use will be restricted to imaging cancer metastases in a only a few organs such as the lung, because there is a high uptake by normal stem cells at sites such as liver and bone marrow.

The relatively small numbers of 'resistant' or cancer stem cells within a tumour represents a further challenge to biomarker sensitivity and whole body imaging. Potential cancer stem cells may constitute $<1\%$ of the tumour population. These cells may already be in the circulation, thus reducing the likelihood of identification by the biomarker. Even if the imaging probe has a sufficiently high specific affinity to bind to the target, significant signal amplification is likely to be required in order to detect minimal target concentrations (typically in the nano- to pico-molar range).[17] Imaging strategies and methods to amplify target signal are discussed in a subsequent section (see section 4.6 *Imaging drug resistance mechanisms including cancer stem cells*).

2.2 Spatial heterogeneity issues

Further challenges are faced in the attempt to image tumour biological responses at a microscopic scale, which will inevitably introduce another level of heterogeneity *i.e.* between individual tumour cells. Furthermore, these imaging techniques have a limited depth of penetration and do not inform on whole body distribution. There is scope to link whole body imaging (*e.g.* PET–CT) to imaging of pathological mechanisms within the tumour cells at a nanometre scale. The enabling technologies linking these two imaging scales will include image-guidance by the co-registration of different images (*e.g.* PET and ultrasound (US)), to improve the current accuracy of sampling tumour-infiltrated lymph nodes, for instance. Image-guided biopsy may complement whole body imaging by improving the accuracy of assessment of response and recurrence, but is invasive. Tumour sites exhibiting poor response to therapy may be biopsied to define whether these cells exhibit a clonal change or a change in receptor expression. For instance, the difference or discordance in protein expression (*e.g.* HER2 status[18]) on cancer cells between the primary tumour and distant metastatic sites may correlate with a differential sensitivity to treatment (to be expanded on further under section 4.2 *Use of imaging to characterise tumour heterogeneity*).

Cancer patient management is guided by the classification of tumours into a variety of subtypes, representative of their pathology and stage, as described by light microscopy, biomarkers derived from antigen-specific immunohistochemistry, mutation and cytogenic analysis, and gene microarray data.[19] However, intratumour spatial heterogeneity may reduce the validity of this categorization. For example, nuclear polymorphism represents one of several characteristics used to determine grade in both invasive ductal carcinoma (IDC) and *in situ* breast cancer. Yet the commonly used grading systems do not recommend a minimum proportion of nuclei that need to be classed in the most marked pleomorphism group. How representative this is of the tumour as a whole is arguable. Conventional grading according to the modified Scarff–Bloom–Richardson method assigns a score depending on the highest level of nuclear atypia. Furthermore, detailed analysis and subclassification of entire DCIS lesions, by immunohistochemistry and microarray analysis, showed intratumoural biological diversity in 46% of all samples.[20] It is likely that histopathological analysis leads to an underestimation of the total intratumour heterogeneity as only a small percentage of the tissue is examined. The use of endoscopic ultrahigh resolution optical coherence tomography/microscopy (resolutions of <4 μm axial and <2 μm transverse)[21] is one of the imaging solutions that has been used to overcome this issue of inadequate tumour sampling.

P. A. Ellis

Professor Paul Ellis studied medicine at Otago University in New Zealand before completing his fellowship in Medical Oncology and his postgraduate Doctor of Medicine research degree at the Royal Marsden Hospital in London. He is currently Medical Director for the South East London Cancer Network. His major breast cancer research interests include working with Professor Tony Ng on the clinical application of optical proteomics and novel clinical research strategies in the adjuvant and neoadjuvant setting.

T. Ng

Tony Ng is the Richard Dimbleby Professor of Cancer Research ⟨http://www.dimblebycancercare.org/⟩, King's College London. He has a mix of training/expertise in medicine, immunology, cancer cell biology, biochemistry, optical imaging and cell biophysics. Using FRET and FLIM techniques, his laboratory has established, in live and fixed tumour cell systems (including xenografts), imaging-based methods that can monitor post-translational modifications and protein interactions, both in space and time. By combining imaging with bioinformatics and network modelling, we are now adopting a multidisciplinary approach to understand the cancer metastatic process and its immunological control.

Although molecular imaging may help delineate intra- and inter-tumour heterogeneity, these findings may create challenging clinical implications. For example, the smallest volume of the tumour expressing the imaged target which may warrant a change of treatment, and the implications of determining the molecular profile of the biopsied material from *e.g.* the secondary site, are issues which will have to be tackled in this context, as we move towards an era of multimodality and multi-scale cancer imaging.

2.3 Combining imaging of different modalities and (length) scales to follow treatment response

An early potential role for molecular imaging in cancer therapeutics is the measurement of tumour response to anti-cancer drugs. Current technologies are limited as the unit of response assessment is anatomical (CT/MRI/US) or a measure of metabolic activity which may be non-specific to drug activity (^{18}F-FDG-PET). The imaging biomarker should be able to delineate established 'on target' drug effects *in vivo*, so that treatment efficacy and response may be assessed. The presence or concentration of a molecular target is not necessarily a read-out of target activity, which is more accurately depicted, in the case of the HER receptor protein-tyrosine kinases, by protein dimerisation, which in turn leads to phosphorylation and signal transduction *via* a variety of intracellular signalling cascades.[22] Except for one or two recent examples,[23,24] molecular parameters that delineate protein target activities, such as protein dimerisation, phosphorylation and other intracellular signalling events, cannot be obtained by whole body imaging and are best studied by specialised cellular and tissue imaging.[25–29] On the basis of our and other colleagues' research findings in the HER field,[26] we maintain that for monitoring clinical response to therapies, molecular imaging would need to take into account the various processes of receptor activation, (*e.g.* ligand binding and dimerisation, which occurs at a nanometre lengthscale) in order to provide an accurate, functional read-out of drug efficacy. One of the key contributions we wish to highlight is our attempt to link these nanometre scale protein oligomerisation/interaction events (nanoscopy) to whole body imaging. Repeated imaging by various modalities may be necessary at different time points to obtain surrogate markers for treatment response, for instance in a neoadjuvant trial setting. However, this imaging approach may incur both financial costs and/or radiation dose concerns (for whole body imaging) as well as the requirement for repeat access to cancer tissues or cells from patients (for nanoscopic analysis) (discussed further in section 2.5 *Radiation and financial issues*).

A combination of imaging techniques, such as CT and PET or MR and PET may help delineate several different pathways sequentially or simultaneously. For example, clinical trials have demonstrated significant modification and improvements to external beam radiotherapy planning with the use of CT–PET imaging, as discussed below (4.1 *Combination strategies*). However, further work is required prior to routine incorporation of this modality into treatment planning. The greater challenge is in the incorporation of radiotracers other than FDG into treatment planning. ^{18}F-FDG-PET scanning has established benefits in staging disease, as exemplified by numerous studies in cervical cancer, lung cancer, intracranial tumours and in assessing lower gastro-intestinal recurrence.[30]

^{18}F-FDG-PET has also been shown to be of benefit in the early assessment of response to therapy and as a prognostic marker for survival, *e.g.* for NSCLC, oesaphageal cancer and lymphoma.[31] The initial assessment of tumour uptake using a semiquantitative uptake value (SUV) is of interest as a predictor for individual patient survival despite varying chemotherapy regimes.[32] Molecular imaging of tissue material from original biopsies may provide useful prognostic and predictive information on tumour biology which may relate to SUV.

Regardless of the issues surrounding use of combinatorial imaging modalities discussed thus far, a further ubiquitous challenge is present: the appropriate choice of biomarker for the diagnostic need. This will most likely vary between different tumour types and may even vary between different patients. Until recently *in vitro* basic biological research has established the mainstay of defining pathological biochemical and gene expression pathways. Molecular imaging holds the promise of evaluating physiological regulations of these pathways within their micro-environment. However, many different proteins are likely to be involved in tumour dynamics. It is not possible to image all those involved and therefore we must devise a strategy to elucidate key 'nodes' within these networks for evaluation in the patient. *In vitro* characterisation of protein–protein interactions has been integrated to build signal networks to model carcinogenic pathways or response to drug treatment, for example for EGFR.[33] 'Nodes' within these networks define key pathways which are integral for carcinogenesis or as a target for therapy. These networks may be used to generate prognostic molecular pathways which can be interrogated *in vivo* using molecular imaging, as discussed below (section 5.5 *Signalling networks to identify optimal drug combinations*).

2.4 A specific challenge in clinic-difficulties with quantification of images

The quantification of imaging signals requires careful consideration. The measured ^{18}F-FDG signal is the sum of 3 components: trapped intracellular ^{18}F-FDG, as well as the contribution from un-trapped ^{18}F-FDG in intracellular and intravascular spaces. In particular the last two components are strongly related to flow related effects.[34] The perfect biomarker for PET based research would be a radioactive tracer that is not rapidly metabolised and is trapped in the tumour or tumour environment, thus increasing its signal with time. Unfortunately the perfect marker does not exist. For instance, with a marker such as fluorothymidine, significant metabolism occurs such that debate exists as to whether correction for the metabolites is required to assess proliferation, the function that is being measured. This also raises the question as to whether visual assessment, semiquantitative assessment or true quantitative assessment is needed. Full quantitation increases the complexity of the examination, often requiring the acquisition of an input

function and scaling this input function to arterial blood radioactivity measurements. If the tracer is metabolised these measurements require correction for the amount of the metabolised product, thus altering the shape of the input function. Most PET centres do not have this ability. Therefore, in order to translate research into routine practice, the technique needs to be simplified, using visual or semi-quantitative measures *e.g.* semiquantitative uptake values. Even for these simplified measurements standardised quality control (QC) and quality assurance (QA) is essential in order to enable different centres to assess the data using a common method. PET–CT has made major strides in establishment of common QA/QC for clinical trials with FDG within Europe.[35] These guidelines have provided a basic standard, but for more complex studies, the level of QA and QC requires escalation beyond these criteria.

Further issues regarding the quantification of imaging signals are faced within multinational biomarker studies. The Society of Nuclear Medicine in the United States of America (USA) has adopted similar guidelines to Europe. However, even within Europe, where there is a purported common European Clinical Trials Directive, the application of the directive is variable. This particularly applies to the investigational medicinal product dossiers required as part of the clinical trial authorisation for new radiotracers. The research and development process in the USA is different and leads to difficulties developing major biomarker studies for patients around the world.

These limitations for PET–CT data acquisition are being addressed such that pan European studies are carried out with data transfer to either a central facility for Europe or to "core" labs in individual countries, thus enabling multicentre research with FDG. Data quality is improved further with attention to detail in image processing methods, data acquisition, phantom data and daily, monthly and annual QC. The quantification of alternate tracers to FDG depends on the manufacturing sites available and the complexity of the image analysis to be performed.

Quantification from CT and MRI techniques is also a challenge. The signal of both DCE-CT and DCE-MRI is the sum of both intravascular and extravascular contributions, and dependent on flow and rate of vascular leakage. The signal of DW-MRI is affected by intravascular flow, the extravascular space volume, presence of macromolecules, and cell density.[36] Kinetic modelling approaches used for DCE techniques may allow quantification of this signal but make assumptions that may not necessarily hold in all cancer types or normal tissue. Measurement robustness remains an issue; this is affected by acquisition technique, particularly where signal to noise is reduced, though less so where a percentage change is being measured rather than absolute values. A further challenge is translating this to the whole body level. The coverage of DCE techniques depends on spatial resolution and temporal resolution, *e.g.* a typical coverage of 4 cm is achieved for a temporal resolution of less than 3 s for DCE-MRI for a single sequence.[37] Whole body DW-MRI is being assessed for staging and response assessment but quantification remains exploratory.

2.5 Radiation and financial issues

Imaging based on ionising radiation, such as X-ray, CT, and PET has a defined cancer risk and repeated imaging for pharmacodynamic end-points may lead to unacceptable levels of radiation exposure. However, this risk is still likely to be small when related to the overall lifetime risk of cancer in a normal population of 1 in 4 and the long term risks of chemotherapy and radiotherapy. Clinical radiation experts are cognisant of the issues related to radiation burden and in systems with financial constraints, keep a tight control over the amount of imaging performed. Furthermore, there is constant review, alongside manufacturers, of dose reduction strategies to achieve the same result. Patient acceptability and feasibility for repeated imaging must be paramount, and assessment of such must be included within the design of imaging clinical trials. The number and type of imaging interventions required must be rationalised in order to avoid these patient and financial costs. Cumulative radiation dose must be calculated for the entirety of the proposed treatment regime for modalities such as CT and PET which utilise ionising radiation. The radiation dose may be tempered in a number of ways.

A more targeted approach appropriate to the therapeutic effects should be considered. For instance, the efficacy of external beam radiotherapy is attenuated in areas of tissue hypoxia. Areas of low oxygenation undergo less necrosis on treatment as radiation-induced DNA damage is reliant upon oxygen. Hypoxia imaging, with ^{18}F-FMISO has already been shown to predict the response to radiotherapy in head and neck and NSCLC patients, and may play a role in the future in delineating disease for radiation boost, or reducing radiotherapy treatment in areas where it is likely to be ineffectual.[38] It is also possible that hypoxia imaging agents could be used to assess whether an improvement to tissue oxygenation has been achieved by an intervention, thus reducing the requirement for a dose boost.

The use of more specific imaging strategies for efficient response assessment should also be considered as alternatives to CT for anatomical response, in order to reduce total radiation dose. If ionising radiation imaging strategies are to be integrated into clinical practice, dose reduction strategies should be employed to maintain as low a radiation dose as possible. The use of lower injected activity and longer imaging times may reduce radiation dose from PET with the same end diagnostic result. The biologic effect of radiation dose is measured in millisieverts (mSv) and is calculated by multiplication of radiation dose to organ, relative biological effectiveness and a tissue weighting factor. The radiation dose for most fluorine labelled tracers using 3–400 MBq is approximately 8 mSv for PET and 10 mSv for a body CT. The risk of inducing fatal cancer is 0.05/Sv or for a standard FDG PET 18 mSv scan, is approximately 1 in 1000 ($18 \times 0.00005 = 0.0009$ or 1 in 1000). This figure has to be related to a 1 in 3 natural lifetime risk for cancer. Cancer patients are at a higher lifetime risk for secondary malignancies due to anti-cancer therapy, *e.g.* radiation from external beam and internal delivery, and chemotherapy. The radiation risk should be weighed up against the potential benefit of imaging.

Justification of the use of radiation in molecular imaging for routine surveillance is equivocal, and is lacking for screening.[39] An appropriate evidence base must be established for the imaging intervention to detect treatable disease at an early stage and/or improve patient outcome, over and beyond the risk of secondary malignancy associated with the radiation. These databases have yet to be established for novel imaging strategies such as molecular imaging/imaging with novel PET probes.

Affordability and availability are two further challenges to the integration of molecular imaging to clinical practice. Nuclear imaging with PET is one of the most developed modalities for molecular imaging, and may be eminently translated to the clinic, due to the established use of PET imaging in lymphoma and NSCLC, for example.[40,41] However the routine use of PET imaging in a variety of tumour types for diagnosis or staging is not supported by evidence from randomised controlled trials (RCT), let alone the use of PET for screening. The current standard cost for a whole body ^{18}F-FDG PET scan is high; approximately £1000 in the UK. If molecular imaging utilising PET is to be integrated into clinical practice, this may entail multiple scans at an early stage in disease, thus increasing costs exponentially. Although a cost-benefit analysis is preferable, in reality, it is difficult for such interventions which may unpredictably change cancer therapy, and for which there are few RCTs to provide an evidence base.

The use of molecular imaging to select appropriate initial therapy and accurately assess disease response has the potential to reduce current costs significantly. For instance ineffectual drugs may be stopped early, saving not only the drug cost, but also producing health benefits in terms of drug toxicities, quality of life, in-patient admissions, and may even allow patients to return to work. For example, ^{18}F-FDG-PET scanning has been shown to improve selection of patients for hepatic surgery of colorectal liver metastases.[93] This study demonstrated a risk reduction in the number of futile laparotomies from 45% to 28% using PET–CT compared to CT, potentially saving costs of surgical interventions, inpatient stays and patient morbidity. Further large RCTs are required to calculate the cost benefit of carrying out PET scans, especially as many of the imaging modalities discussed thus far are research technologies. The ongoing Risk Adapted Therapy for Hodgkin's Lymphoma trial and a Cancer and Leukaemia Group B study are being carried out to address the benefit of PET imaging in reducing treatment intensity compared to standard high dose therapy or escalating therapy in those patients not responding to treatment, based on the FDG PET result. Data from studies such as these may help quantify the cost benefit of PET imaging. Within these studies, the acceptability and feasibility of multiple imaging for the patient must also be addressed. Molecular imaging with PET holds great promise in optimizing cancer therapy, especially in the arena of surveillance and risk-adapted therapy.

In the following sections, we discuss examples of *in vivo* and *in vitro* molecular imaging modalities within the context of the challenges described above.

3. Various established and investigational imaging methods

Current imaging systems are based on the interaction of electromagnetic radiation or ultrasound waves with body tissues or fluids. High frequency electromagnetic radiation in the X-ray spectrum is ionising and may be tumourigenic in itself.[94] PET and nuclear medicine imaging systems have higher functional sensitivity compared to magnetic resonance imaging (MRI) which is more sensitive than X-ray systems such as CT.[9] Examples of established and novel imaging techniques are summarized in Table 1.

Until recently modalities such as CT and MRI have been used in diagnosis, staging and assessment of response to treatment by measuring the volume of disease. Gross macroscopic changes lag in time following alterations at the molecular level.[95] The Response Evaluation Criteria in Solid Tumours (RECIST) criteria, based on unidimensional tumour measurements, is the established method for assessing disease burden in clinical trials. However, structural changes may be non-specific, *e.g.* due to inflammation or malignancy. For example, the efficacy of cytostatic targeted therapies cannot be assessed on structural data alone.[96]

A combined approach, integrating the metabolic sensitivity of FDG PET with the anatomical spatial resolution of CT, is increasingly used in clinical practice. This has been validated for use in staging, detection of residual disease, and to assess response to treatment.[97] Using NSCLC as an example, PET–CT has improved staging accuracy, reduced futile thoracotomy rate and improved radiotherapy planning.[98] Recently, Positron Emission Tomography Response Criteria In Solid Tumours (PERCIST) have been introduced[99] which combines the quantification of anatomical changes (RECIST) with those developed by the EORTC PET response group.[100]

Although CT and MRI are mainly static techniques, emerging techniques, such as dynamic contrast enhanced (DCE) CT,[101] DCE-MRI[102] and DW-MRI have allowed quantification of vascularization and water diffusion. Over the last decade, DCE-CT and DCE-MRI techniques have been explored in Phase I and II studies of anti-angiogenic and vascular disrupting agents to provide evidence of a mechanistic, anti-vascular effect.[103] Studies employing DW-MRI for response assessment are emerging.[104] Multi-parametric approaches for example with MRI encompassing information on anatomy, perfusion, and cell density and proliferation has the potential to offer earlier, and more precise, information on treatment response in the neoadjuvant setting than RECIST.[105]

4. Current state-of-the-art cancer imaging applications

4.1 Combination strategies

In clinical practice, the combination of various modalities such as PET and CT, have been shown to improve oncological imaging, especially for diagnosis, staging, response assessment, guiding biopsy and radiotherapy planning. In the USA, PET–CT is now included in NCCN practice guidelines in 21 cancers. In

Table 1 Current and promising research imaging modalities

Imaging modality	Contrast agent	Examples of therapeutic intervention assessed	Benefits
X-Ray based imaging			
Computed tomography (CT)	Density of varying body tissues (variable absorption of X-Rays)	All therapies, and routinely used in clinically trials as end-point (RECIST criteria). Used for image-guided biopsy and radiotherapy planning	Routine practice, widely available, standardized. Good spatial resolution
Dynamic contrast enhanced (DCE)-CT[42,43]	Iodinated agents (time-to-peak enhancement correlates with tumour perfusion and vascular permeability)	Anti-angiogenic or antivascular agents, *e.g.* non small cell lung cancer (NSCLC)	Assesses on target drug effects, can be incorporated into readily available technology (CT)
CT colonography[44]	Tissue density (X-ray) and contrast agents	Colonic screening -detects polyps >10 mm	Less invasive compared to colonoscopy, suitable for elderly patients, concomitant staging
Full field digital mammography[45]	Tissue density (X-ray)	Used as screening tool for breast cancer, in combination with computer assisted detection	Reduced radiation dose, improved sensitivity for dense breasts, tomosynthesis (3D visualization)
PET			
^{18}F-FDG-PET $\pm$ CT	Uptake of ^{18}F-FDG, analogue of endogenous glucose	Response to imatinib in gastro-intestinal stromal tumours (GIST), prediction of response to chemotherapy in NSCLC, oesophageal and colorectal cancer.[46–48] Prognostic capacity in lung, oesophageal and thyroid cancer[41,49]	Clinically approved. Quantification of tumour metabolic activity possible by SUV.[50] Predictive of treatment response with non-cytotoxic agents, *e.g.* imatinib. Improved biomarker for clinical response compared to RECIST
^{18}F-FDG-positron emission mammography (PEM)	Uptake of ^{18}F-FDG	Identification of DCIS *vs.* invasive breast cancer	90% sensitivity for tumours less than 1 cm in size[51]
^{18}F-FMISO-PET & ^{18}F-FAZA (Hypoxia imaging)	^{18}F fluoro-misonidazole nucleoside (^{18}F-FMISO), and ^{18}F-fluoroazomycin arabinoside (faster clearance compared to ^{18}F-FMISO)	Predicts treatment response for radiotherapy in NSCLC and head & neck cancer,[38] clinical imaging of head and neck patients.[52]	Identifies hypoxic tumour tissue which is resistant to DNA damage by radiation or chemotherapy.
^{18}F-FLT-PET (Proliferation imaging)	3′-deoxy-3′-^{18}F-fluorothymidine (FLT) to infer rate of cellular proliferation	Response to chemotherapy in breast cancer and radiotherapy in pre-clinical models[53]	Non-invasive measurement of proliferation, especially relevant for non-cytotoxic drugs. (correlates with Ki-67)
^{18}F-annexin V-PET (Apoptosis imaging)	^{18}F-annexin V	Apoptosis imaging in animal models[54]	Lower uptake in the liver, spleen and kidneys compared to ^{99m}Tc-annexin V
^{18}F-FES-PET	^{18}F-fluoro-17βoestradiol	Response to tamoxifen in breast cancer[55]	May be able to delineate differential expression of oestrogen receptors in primary *vs.* metastatic deposits
Acetate PET imaging	^{11}C-acetate	Well-differentiated hepatocellular cancer, brain carcinoma[56]	Labels relevant endogenous compounds to monitor intrinsic biological processes. Low renal excretion, may be useful in urological cancer.
^{124}I-PET	^{124}I-antibody fragments, *e.g.* anti-HER2 antibodies and ^{124}I-annexin V	Anti-HER2 labelled diabody used to image HER2 + ve xenograft[57]	Longer half-life (100.3 h) facilitates imaging, matches biological half-life of antibody fragments used for labelling, and allows imaging at late time-points
^{89}Zr-PET	^{89}Zr-antibodies, *e.g.* ^{89}Zr-U36(anti-CD44 monoclonal antibody)	Stage and detect lymph node metastases in head and neck cancer patients[58]	Long half-life (78.4 h), as above. May be better than ^{124}I for internalising antibodies as ^{89}Zr remains in the cell
^{68}Ga-PET	^{68}Ga-peptides, cancer stem cells and antibodies, *e.g.* ^{68}Ga-Fab2-herceptin	RGD peptides (bind to $\alpha_v\beta_3$ integrins) image angiogenesis.[59] ^{68}Ga-Fab2-herceptin used to monitor HER2 as a target for Hsp-90 inhibitors, in clinical phase I trials[60]	Non-invasive monitoring of angiogenesis. Clinical application in patients with HER2 + ve tumours.
^{64}Cu-PET	^{64}Cu-vascular endothelial growth factor	Imaging of angiogenic vasculature[61]	Images VEGF, angiogenesis regulator, and monitoring of response to VEGF targeted drugs.
Radiolabelled drugs	^{18}F-desatinib, ^{18}F-paclitaxel, tamoxifen, fluorouracil and ^{13}N-cisplatin[62]	Imaging of prostate xenografts with ^{18}F-desatinib.[63] Pharmacokinetics of labelled chemotherapeutics: biodistribution, metabolism, response, dosimetry.	Ideally combines treatment and imaging. May be used for the study of drug pharmacokinetics

Table 1 (*continued*)

Imaging modality	Contrast agent	Examples of therapeutic intervention assessed	Benefits
MRI			
MRI	Tissue relaxivity	Used for locoregional staging *e.g.* breast cancer, rectal cancer for staging and surgical planning. MRI is superior to US/mammography for assessing response to treatment[64]	Excellent soft tissue resolution, Non-ionising radiation (recommended for patients at high-risk of radiation induced DNA mutations, *e.g.* BRCA1&2[65])
DCE-MRI	Ga chelates (kinetic modelling assesses K_{trans}, k_{ep}, v_e, v_p)	Predicts response to chemotherapy in breast cancer[66] and chemoradiotherapy in rectal tumours.[67] Assess effects of anti-angiogenic agents in early trials[68]	Dynamic studies possible utilizing a widely-available technology
Contrast enhanced (CE)-MRI	Targeted Ga chelates binding to cell surface markers of angiogenesis (*e.g.*VEGF, $\alpha_v\beta_3$)[69]	Assess pre-clinical effects[70]	Non-invasive assessment of angiogenesis
CE-MRI	Ultra small particle iron oxide (USPIO) accumulation in macrophages	Evaluation of lymphatic drainage for detection of micrometastasis, *e.g.* breast, bladder & prostate cancer[71,72]	100% sensitivity for LN mets in breast cancer (in combination with FDG-PET)[71]
CE-MRI	Targeted USPIOs, *e.g.* to annexin V,[73] HER2 receptor[74] or stem cell markers[75]	*In vitro* and pre-clinical *in vivo* demonstration of targeting agent only.[76]	Non-invasive assessment of key metabolic processes in oncogenesis, and potential to assess response to cytotoxic chemotherapy or targeted agents.
Diffusion weighted imaging (DWI)-MRI	Water diffusion[77]	Biomarker of response to chemoradio-therapy, time to progression and overall survival in malignant glioma,[78] response to neoadjuvant chemotherapy in breast ca[79]	Whole body DWI-MRI may compete with FDG-PET for evaluation of soft tissue and bony disease.
Blood oxygen dependent MRI (BOLD MRI)	Blood oxygenation	Surgical planning in cranial tumours[80]	Non-invasive imaging of tumour hypoxia, especially useful intra-cranially[81]
MR spectroscopy			
Proton MRS	Proton $(H)_1$, allows quantitation of tissue metabolites containing $(H)_1$, *e.g.* choline, amino acids, nucleotides, lipids	Prognostication and assessment of residual disease in gliomas.[82] Pilot studies in staging breast and prostate cancer[83]	Improved specificity and resolution, especially when combined with MRI.
Fluorine Spectroscopy	Fluorine ^{19}F spectroscopy allows quantification of exogenous ^{19}F containing molecules[84]	Measurement of chemotherapy response[85]	Quantitative information of drug uptake
Spin hyperpolarisation	Hyperpolarised metabolites of labelled proteins.*e.g.* ^{13}C-pyruvate, acetate or urea	Pre-clinical *in vivo* measurement of chemotherapy induced cell death using ^{13}C-pyruvate[86]	May be useful for non-specific measurement of treatment response
Optical imaging			
Bio-luminescence	Overexpressed luminescent protein, *e.g.* luciferase	Relapse and metastases in prostate cancer xenograft models[87]	Very sensitive with high spatial resolution.
Optical coherence tomography (OCT)/ microscopy (OCM)	Varying reflection of low-coherence light from tissues	Differentiation of DCIS from invasive malignancy intra-operatively[88]	Image resolution of <1 micron, represents tissue microarchitecture comparable to histopathology
Fluorescence imaging	Molecular probes which may fluoresce in presence of target protein	Matrix-metalloproteinase activity in murine models[89]	Functional imaging of oncogenic process, can be translated to MRI
Förster resonance energy transfer (FRET) assays[28,29]	Interacting fluorescent probes	Effect of chemotherapy on caspase activity,[90] multiphoton endoscopy[91]	Highly specific method of functional imaging
Ultrasound			
Conventional ultrasound (US)	Echogenicity of tissues	Most commonly used in breast cancer detection, staging, and for image-guided biopsy	Inexpensive, widely available, non-ionising radiation
US + microbubble technology	Contrast microbubble agents	Detection of tumour angiogenesis in animal models[92]	Enhanced signal from tumour vasculature
Nuclear medicine			
Conventional radiolabelled ligands	^{131}I, ^{111}In, ^{99m}Tc, ^{67}Ga	Neuroendocrine imaging with *e.g.* MIBG, or radiolabelled octreotide[13]	Ligand specificity to receptors overexpressed on tumour
β-Particle emitter	^{90}Y	Peptide receptor radionuclide therapy[11]	Direct translation of imaging ligand for therapeutic benefit.

radiotherapy PET–CT has been integrated into radiotherapy planning for NSCLC with a modification in the definition of gross tumour volume (GTV) treated and improvement in inter-observer variability.[106] Similarly, PET–CT was found to improve GTV definition compared to CT alone for patients with pancreatic carcinoma, potentially reducing the risk of geographical misses.[107] In the latter study both scans were acquired separately and the data was co-registered.

Various co-registration software programs have been written in order to register pre-procedural scans with real-time scanning, as discussed for TRUS–MRI of the prostate (section 5.2). Briefly, matching landmarks on both studies are graded, either manually, automatically, or both, in order to match real-time needle positioning to anatomy from prior images. Similar software application to PET–CT guided biopsy of intra-abdominal lesions has been to shown to be feasible.[108] This area is particularly difficult to characterise due to motion artefacts of peri-diaphragmatic structures, *e.g.* liver, due to respiratory effort. Non-rigid algorithms can accommodate this movement but require powerful computers and are labour intensive for routine procedures. Tatli *et al.* used rigid algorithms and achieved technical feasibility for biopsy of liver lesions.[108] Finally, in the case of PET–MR image fusion in soft tissue sarcoma which lacks conspicuous anatomical features and deviates from the rigid-body model, point-based PET–MR registration using external markers is practical, reliable and accurate to within approximately 5 mm towards the fiducial centroid.[109] Thus accurate targeting for biopsy is facilitated by the co-registration of multiple image modalities.

Fundamental improvements in the way we apply imaging in clinic can potentially be achieved by combining imaging modalities at different resolutions. For instance, MRI-guided clinical staging and presurgical planning may in the future be combined with intra-operative fluorescence-guided surgery, through the development and approval of nanoparticles that are dually labelled for *in vivo* fluorescence and MR imaging of proteases.[110] Other examples include nanoparticles that contain a radionuclide (*e.g.* ^{18}F) and a far red fluorochrome; with the latter being amenable to imaging with fluorescence-mediated tomography *in vivo*, and at microscopic (sub-micron) resolution *ex vivo*.[111] Promising technologies have demonstrated the feasibility of combining three different imaging modalities, PET, MRI and optical imaging.[112] This study demonstrates the advantages of combining these strategies, *e.g.* 50 times improvement in soft tissue sensitivity compared to conventional MRI, thus drastically reducing injected tracer volumes and rigorous probe validation.

4.2 Use of imaging to characterise tumour heterogeneity

Disseminated tumour cells may exhibit a very different phenotype to that of the primary tumour. They may consist of stem cells, which are resistant to treatment or may express antigens which allow escape from immune surveillance in order to seed at a distant site and establish metastases. The assessment of tumour heterogeneity becomes imperative at metastasis, as differential protein expression across tumour deposits may have implications on the treatment regimes used.

One clinical example pertains to the overexpression of the HER2 receptor in a variety of tumour types, the most prominent of which is breast cancer. It is overexpressed in approximately 25% of patients and is associated with a poor prognosis.[113] A number of therapeutic interventions have been designed in order to block the HER2 receptor, including trastuzumab and small membrane-penetrating molecules that compete with ATP at the intracellular tyrosine kinase domain, *e.g.* lapatinib. The decision to employ HER2 targeted treatments depends upon overexpression of the receptor, as detected by immunohistochemistry (IHC), or gene amplification as determined by fluorescence *in situ* hybridization (FISH), usually on primary tumour tissue alone. Comparison of the HER2 status of primary and metastatic lesions by IHC reveals significant discordance: 127 out of 342 patients, 90 having a HER2 positive tumour but HER2 negative metastases, and 37 having a HER2 negative primary tumour but HER2 positive metastases.[114] A similar series has observed heterogeneity for HER2 amplification within the primary tumour site.[115] This discordance between primary and metastatic tumour site could alter management of metastatic disease but is often not uncovered due to the difficulty in obtaining repeated, invasive biopsies on patients with metastatic disease. An imaging modality which could characterize all systemic lesions would greatly aid effective patient treatment.

Radiolabelled tracers to the HER2 receptor have been developed by labelling monoclonal antibodies, antibody and peptide fragments for PET, SPECT and MRI imaging. Although full sized antibodies have been used, they are slowly cleared from the bloodstream due to their size. Thus labelled fragments are being developed.[116] The most successful of these to date are HER2 Affibodies and a fragment of trastuzumab labelled with ^{68}Ga using DOTA (1,4,7,10-tetraazacyclododecane-1,4,7,10-tetraacetic acid) as the chelating group.[117] PET imaging is preferred to SPECT as it is about an order of magnitude more sensitive, detecting molecules in the pmol L^{-1} range. Affibodies are small non-immunoglobulin-affinity proteins which are proven tracers for molecular imaging.[118] ^{111}In- and ^{68}Ga-labelled HER2 affibodies have been used in patients to visualize HER2 positive metastasis using PET and SPECT imaging, in 9 out of 11 locations.[119] Although this result is preliminary, the tracers were well tolerated and comparable to ^{18}F-FDG-PET. One of the patients examined was on trastuzumab therapy, which did not interfere with radioligand binding.

These examples illustrate the feasibility of HER2 receptor imaging *in vivo*. However, integration of this information into patient management represents a further challenge. For instance, high uptake of ^{111}In and ^{68}Ga-affibodies in the kidneys and liver exclude these important metastatic sites from functional imaging. The spatial resolution of the images is sufficient to detect whether a HER2-positive metastasis is present or not, but not to delineate spatial heterogeneity within that sample. The presence of an established targeted therapy such as trastuzumab indicates that HER2 detection, either in a primary or metastatic site, warrants treatment with the targeted drug. However, the proportion of HER2 receptors detected within the tumour may be difficult to standardise and quantify *in vivo*, due to the limits of resolution with PET imaging. Current histopathological recommendations define HER2

postivity as greater than 30% of cells exhibiting the receptor on immunohistochemistry, and equivocal if greater than 10%.[120] However, until these guidelines were published, controversies existed in this established field regarding standardised operating procedures, and proficiency testing within the laboratory. The direct translation of this definition to a 3 dimensional *in vivo* sample is fraught with further difficulties. Even if potential HER2 receptor positivity is defined as 10% of the tumour volume on imaging, questions still remain. Does this volume refer to the total tumour volume within the patient or specifically to the site where the receptor is detected? Furthermore, the clinical significance of the volume of HER2 detected is not known as cancer databases have quantified HER2 positivity from IHC or fluorescence *in situ* hybridisation (FISH) from tumour biopsies thus far. Large scale observational clinical studies are required to assess the prognostic significance of varying levels of HER2 receptor detection within a tumour sample on imaging, prior to establishment of guidelines regarding treatment decisions.

By introducing our combined modality and multiscale imaging approach, biological heterogeneity that exists both within primary tumours and between primary and metastatic tumours becomes a significant challenge for rationalising targeted therapies. For example, questions such as the smallest volume (number of voxels) of the tumour expressing the imaged target that persists in a patient following targeted therapy, to warrant a change of treatment, have yet to be defined in this context. Having set out to describe the advent of novel imaging techniques, *e.g.* both radionuclide-based and nanoscopic imaging (section 5) of HER receptor, applicable to whole body and cells/excised tissues, we do not yet know the full extent of the heterogeneity issues that may be brought to light by these new techniques. It would be crucial in the future, however, to take into account the additional information obtained using these techniques and then validate their use in informing treatment response or possible patient stratification.

4.3 Drug pharmacokinetics and pharmacodynamics

Drug pharmacokinetics (PK) describes the effect of the body on a drug, namely, liberation, absorption, distribution, metabolism, and excretion. Pharmacodynamics (PD) describes the effect of the drug on the body, including therapeutic effects and unwanted toxicities. These properties describe two key factors in drug therapeutics; namely, how much of the drug is reaching its target, and whether it is fulfilling its purpose. Definition of the relationship between PK and PD is essential to the rational delivery and targeting of therapeutic agents, especially for those drugs with established molecular effects. Temporal delineation of drug pharmacodynamics can inform on drug response, appropriate drug dosing regimens and can provide an early assessment of resistance to therapy.

Traditional PK endpoints include invasive assessment of drug serum concentration by a variety of methods including liquid chromatography and mass spectrometry, and PD endpoints are assessed on repeated tumour samples or surrogate tissue.[121] However, repeated tumour sample biopsies can be challenging from the practical perspective. Biopsies are invasive, and fixed in time and space. Many sites are not easily accessible *e.g.* intracranial tumours or mediastinal lymph nodes. Repeated invasive biopsies whilst patients are on therapy may confer patient morbidity and are not always acceptable or feasible.

PD endpoints are often defined by the maximum tolerated (MTD) dose, which is determined in phase I clinical trials by exposing sequential patient cohorts to increasing doses of the drug until the toxicities are intolerable. The MTD is described as one dose level below the dose at which intolerable toxicity occurs.[122] Optimal biological dose (OBD) is arguably a more rational phase I trial endpoint in the case of targeted therapies.[123] OBD is defined by PD assessment of effective target modulation, and may be attained at doses substantially below MTD.

The number of targeted novel agents available has increased exponentially over the last decade, but the tools to assess real-time function *in vivo* are awaiting more effective translation to the clinic. Molecular imaging could be used to assess OBD and aid decision-making in terms of appropriate dosing schedule and regimen, thus reducing the need for multiple biopsies. These non-invasive markers could illustrate real-time patient heterogeneity and differential drug sensitivity, both at the drug development phase, and in routine practice.

4.4 Pharmacokinetic and pharmacodynamic imaging biomarkers: potential applications and limitations

PET imaging, of either a directly labelled drug or an isotope-labelled ligand, has commonly been used in the assessment of drug PK and PD.[124] The quantitative nature of PET allows determination of drug concentration in tissue, as low as 1×10^{-12} mol L^{-1}. The radionuclides commonly used for PET, *e.g.* carbon, nitrogen, or fluorine, may be incorporated into almost any drug for tracer synthesis, and the short physical half-life of these tracers results in favourable radiation dosimetry. Chemotherapeutics and targeted drugs have been radiolabelled in order to address their biodistribution and pharmacokinetics, *e.g.* ^{111}In-PEGylated liposomal vinorelbine, ^{64}Cu-DOTA-cetuximab or ^{64}Cu-DOTA-trastuzumab.[125,126] These studies are also known as 'microdosing', or phase 0 studies, whereby less than 1% of the therapeutic dose is administered, so that toxicities are unlikely yet drug half-life, rate of absorption and excretion can be measured on repeat scans.[127] However, the drugs do not achieve therapeutic efficacy, as shown by ^{111}In-PEGylated liposomal vinorelbine in a murine model of colon carcinoma, and as the doses are so low, extrapolation to PK of the therapeutic dose can be difficult. For example, first pass metabolism, gastrointestinal transporter mechanisms, and plasma protein binding can all be very different at such a low dose. The assessment of drug PK *in vivo* remains in the pre-clinical arena. Although clinical translation holds the potential to tailor dosing regimens according to individual patient metabolism, significant further research is required in the pre-clinical arena, for instance, to improve chemical specificity or methods of extrapolation from microdosing studies.

In terms of PD biomarkers, molecular imaging already plays a role in the clinical field. For example, ^{18}F-FDG-PET can be used to predict response to platinum based chemotherapy in patients with NSCLC, as discussed previously.[47] This study

used a non-specific radiolabelled tracer in order to assess tumour burden. However, more specific radioligands are under development. ^{64}Cu-DOTA-trastuzumab and ^{89}Zr-trastuzumab have been used to demonstrate the effects of heat shock protein-90 (hsp-90) inhibition on HER2 expression.[126,128] Hsp-90 is a chaperone for the receptor tyrosine kinase HER2. Inhibition of hsp-90 allows ubiquitination, degradation and down-regulation of this oncogenic protein in tumours over-expressing HER2.[129] This example represents the development of an imaging biomarker to visualise the 'on-target' effects of a drug, and real-time assessment of downstream *in vivo* effects. ^{89}Zr-trastuzumab has been approved for use in humans and has already been trialled in patients with metastatic breast cancer. Therefore, this probe could be translated into the clinical environment.[130] This study included patients who were currently receiving trastuzumab, and the authors did not find that concurrent treatment with the non-radiolabelled drug interfered with detection rates.

However, there are several limitations. This study on metastatic breast cancer patients clearly demonstrated high uptake of the radiolabelled drug in the liver, which precludes the imaging of hepatic metastases. As this is a prime site for metastases from many tumour types, alternative tracer development may be necessary. A general limitation of these tracers is the lack of *in vivo* chemical specificity. A radiolabelled tracer cannot always be distinguished from its radiolabelled metabolites, thus confounding functional biomarker read-out. Accumulation of the tracer in tumour may depend on intrinsic characteristics, such as vascularisation and necrosis, as well as tracer binding, complicating the result. Thus far, molecular imaging has been shown to improve clinical drug response assessment, albeit in a non-specific manner.[48] However, in order to develop imaging pharmacokinetic and pharmacodynamic end-points, extensive clinical evaluation is required in order to assess whether the biomarkers measure drug effects and whether this translates into a clinically meaningful benefit.[131]

4.5 Mechanisms of drug resistance

Cancer cells may exhibit drug resistance due to a variety of mechanisms. Germline factors may contribute and include examples such as polymorphisms in *MDR1*, a gene encoding for efflux transporter *p*-glycoprotein, which limits the access of drugs to the site of action, and mutations in the tumour suppressor gene, *p53* which inhibits apoptosis.[132] Chemotherapeutic agents such as anthracyclines and taxanes are hypothesized to elicit drug resistance *via* mechanisms such as increased drug efflux, decreased drug influx, target modification, drug detoxification or modifications to apoptosis signalling pathways, increased drug inactivation, increased repair of DNA damaged by chemotherapy and enhancement of alternative survival signalling pathways.[133] Alternatively, cancer stem cells may exhibit inherent, epigenetic mechanisms of drug resistance, as discussed in a the subsequent section.[134] Potential imaging biomarkers (both at whole body and subcellular levels) that detect and quantitatively monitor these resistance mechanisms may be invaluable in implementing the concept of personalised medicine.

Currently available systemic treatment for cancer rarely eradicates all disease as exemplified in the neo-adjuvant setting. In a recent study the rate of pathological complete response after neo-adjuvant chemotherapy was quoted as 27% for basal-like, 36% for HER2 positive, and 7% for luminal subtypes of breast cancers.[135] Tailoring the treatment regimen employed according to the molecular mechanisms of drug resistance may improve patient outcome, for both cytotoxics and targeted therapeutics.

4.6 Imaging drug resistance mechanisms including cancer stem cells

P-glycoprotein (Pgp), a transporter protein, is a member of the superfamily of adenosine triphosphate (ATP) binding cassette (ABC) transporters. Pgp maintains chemical homeostasis, especially at protective sites, *e.g.* brain, testes, and can pump cytotoxics out of the cell irrespective of concentration gradient. Therefore it has been of interest as a biomarker for both SPECT and PET imaging.[136] However, Pgp activity is difficult to image directly as ligands are actively extruded from the cell. Therefore, Pgp activity is inferred by measuring the absence of the radiolabeled substrate in a protected site, with or without a Pgp inhibitor. Several radiolabeled drugs, including chemotherapeutics such as ^{11}[C]-paclitaxel and ^{11}[C]-daunorubicin, have been used in animal models but the only drugs to progress to clinical evaluation are ^{11}[C]-verapamil and ^{11}[C]-loperamide. These tracers have been chosen due to intrinsic chemical properties, such as high-signal to noise ratio and low signal contamination by their radiolabeled metabolites.[137] However, none have yet been used in patients with drug resistant tumours. As studies have linked Pgp expression to drug resistance and lower overall survival rates, this imaging approach may be key to assessing its function in multidrug resistant cancer, and thus requires further development.

It is likely that drug resistance of a small number of rare cancer stem cells is naturally present before treatment with anticancer agents. The selective pressure of drug treatment encourages clonal expansion of these cells. Sharma *et al.* examined the effects of supramaximal EGFR tyrosine kinase inhibition in the PC9 non-small cell lung cancer cell line, which carries an EGFR activating mutation in exon 19.[138] Exposure to the EGFR inhibitor, erlotonib at 50 times the treatment dose (IC_{50}) resulted in cell death for the majority of parental cells. The small surviving proportion ($\sim$0.3%) of non-dividing, quiescent cells acquired non-mutational (genetic) resistance to the drug treatment (named drug tolerant persisters, DTPs). The cancer stem cell phenotype was pivotal to survival of erlotonib treatment. All DTPs express the cancer stem cell markers CD133 and CD24, whereas the parental PC9 tumour cells exhibit heterogeneous stem cell marker distribution, which is associated with sensitivity to drug treatment. A synergistic effect of using erlotonib with HDAC inhibitors to eradicate the parental and the majority of resistant DTP cell lines was demonstrated in this study. *In vivo* assessment of the stem cell phenotype and inherent or acquired mutations conferring resistance to treatment, by subcellular imaging, could aid in the rational design of treatment strategy to overcome these mechanisms.

Real-time assessment of resistance is especially important in the stem cell population as the drug-tolerant state may well be reversible. For example, colorectal cancer patients who are resistant to the chemotherapy drug irinotecan may become resensitised to the drug on cetuximab (a monoclonal antibody to EGFR) treatment.[139] A similar phenomenon has also been shown in patients who exhibit primary or secondary resistance to the chemotherapeutic, oxaliplatin. Treatment with cetuximab sensitises these patients to oxaliplatin.[140] These observations suggest a constant state of flux in the prevalence of a variety of resistant 'stem cells'. Repeated biopsies to identify these cells may not be feasible or acceptable to patients. Therefore imaging of the mechanisms involved in the reversible drug-tolerant state, is likely to be key to successful eradication or control of tumour burden.

The development of a drug-tolerant state may be overcome by the use of metronomic dosing schedules. This involves the continuous administration of classic chemotherapy agents at relatively low, minimally toxic doses, with shorter or no drug free breaks.[141,142] Metronomic chemotherapy has been shown to inhibit tumour angiogenesis, but may also positively modulate the immune response against cancer cells and also induce tumour dormancy.[141] Metronomic chemotherapy can be used in combination with conventional chemo-radiotherapy and/or targeted therapy, with positive responses reported in hormone-resistant prostate cancer,[143] recurrent ovarian cancer,[144] and recurrent /metastatic breast cancer,[145] amongst others. Such a dosing schedule may be employed for those tumours in which a high proportion of resistant cells have been demonstrated by molecular imaging. However, metronomic therapy is not yet established practice and further work is required in this field, to, for example, define the number of cells making up the 'resistant population'. This may be hindered by the spatial resolution or sensitivity of the imaging modality as well as tumour heterogeneity, as described above.

Whole body assessment of resistant or stem cell distribution faces many challenges. These cells may be present in various tumour sites in very small numbers, or in the circulation. Whole body, metabolic imaging systems such as FDG-PET are limited in spatial resolution to 2–5 mm, with a high sensitivity (10^{-11}–10^{-12} mol L^{-1}, *i.e.* picomolar).[17] In order to use metabolic imaging to detect stem cells above background noise, the imaging probe would have to bind to several million cells in close proximity. For example, within a 1 cm^3 tumour deposit, one may expect over 1 billion cells. If, for instance, stem cells occupy 1% of this volume, this would entail approximately 10 million cells which may be detected by PET, but only if these cells are within close proximity. If the probe detects innate changes in DNA or mRNA, the number of targets per cell would be reduced drastically to 1–2, or 10–1000 per cell, respectively. It is entirely feasible that the realistic volume of cancer stem cells in the body may fall below the detection limit of whole body imaging.

This challenge may be circumvented in a number of ways. Amplification of the signal emitted from the reporter probe could allow detection of a much smaller number of cells, assuming the probe itself has a high affinity, sensitivity and specificity. The imaging probe itself may be amplified by avidin–biotin amplification or the attachment of large numbers of radioactive molecules to the probe, assuming the probe has a high specific activity.[146] Sensitivity of the probe may be increased using fluorescence dequenching but this imaging modality has not yet been applied *in vivo* for this indication.[147]

Furthermore, with the advent of gene therapy, stem cells have been labelled, transplanted and monitored with non-invasive imaging, in animal models.[148–150] These methods utilise imaging techniques such as MRI with nanoparticles or ^{18}F-FLT PET imaging of non-specific cell processes. Stem cells are identified either at a known location, *e.g.* at sites of transplantation or sites where they are known to reside, such as the subventricular zone of the hippocampus for neural stem cells.[149] The relevant technology for monitoring cancer stem cells *in situ* would require non-invasive imaging of an established stem cell marker or gene transduction with reporter gene technology. Although the latter method has been applied, *in vivo*, *e.g.* for human mesenchymal stem cells in large animals[150] or adenoviral mediated transgene expression in patients with hepatic malignancy,[151] many challenges are associated with this type of technology. The main issue surrounds the logistical and ethical concerns regarding the transplantation of cancer cells into patients, which we do not have scope to fully address here. One example of clinical reporter gene use in a patient with grade IV glioblastoma, treated with cytotoxic CD8+ T cells genetically engineered to express the PET imaging reporter, illustrates an area for potential clinical application.[152] However, this technology is in its infancy and much work is required before general clinical use can be considered.

The identification of established cancer stem cell markers could provide a more readily acceptable assay for identification of stem cells *in vivo*. For example, CD133/prominin, a cancer stem cell surface marker, was identified in mouse xenograft models, using a fluorescent-labelled monoclonal antibody and quantitative fluorescence-based optical imaging.[153] CD 133 is a glycosylated transmembrane protein which loses specific epitopes upon differentiation, thus enabling its use as a cancer stem cell marker for brain tumours, pancreatic, colon, bronchial and prostate cancer amongst many others.[154] Optical imaging of CSCs within subcutaneous xenografts was possible, as confirmed by FACS and immunohistochemical analysis. However, direct translation of this technology for tumours which are not anatomically superficial would be difficult. Although there are several potential methods of identifying CSCs within tumour bulk, those utilising signal amplification of established biomarkers, are most likely to be applicable to clinical practice.

The identification of CSCs poses significant challenges to systemic imaging modalities, partly due to the limit of sensitivity of resolution. Following, we discuss alternative options for imaging at the micro- or nano-metre scale.

5. Protein oligomerisation/interaction imaging—preclinical and clinical applications

5.1 Linking whole body imaging modalities to micro-/nanoscopic imaging of subcellular mechanisms *in vivo*

Attempts have been made to adapt whole body imaging modalities for imaging protein activity and function in tumours. For example, the morpholino-[^{124}I]-IPQA probe was developed to bind irreversibly to the ATP binding site of activated EGFR kinase, but not the inactive form, in order

to demonstrate specifically the active form of this oncogenic receptor *in vivo*. PET imaging established an increased uptake in high EGFR expressing cell lines, in mouse xenografts, compared to low EGFR expressing lines.[155] In addition, by examining the kinetics of the radioactive decay during washout, this technique was shown to distinguish tumour cells expressing a constitutively activated variant of EGFR (EGFRvIII), from its wild type counterpart.

The interrogation of protein–protein interactions at the nanometre scale has been shown with PET imaging of a split reporter in xenograft models.[24] A genetically engineered PET-reporter construct, encoding the herpes simplex virus type 1 thymidine kinase (HSV-tk), is split with the N- and C-termini attached to hypoxia-inducible factor-1α (HIF-1α) and the Von Hippel–Lindau (VHL) tumour suppressor protein, respectively. Interaction between HIF and VHL, leads to reconstitution of HSV-tk, which can be quantified by microPET using radiolabelled probes such as ^{18}F-FHPG and ^{18}F-FHBG. However, as this strategy requires the injection of a genetically engineered construct, it is not yet appropriate for *in vivo* imaging use.

MRI is an alternative to PET imaging at the cellular level. Iron oxide nanoparticles with super paramagnetic properties may be used as contrast agents in MRI as they cause changes in the spin–spin relaxation times of neighbouring water molecules.[156] Surface modifications for conjugation of radiolabeled chemicals or therapeutic agents, are easily carried out on nanoparticles as they have a large surface area. Therefore these particles may be used as contrast agents, or to deliver targeted therapeutics to tumour sparing normal tissue.[157] For example, an IgG antibody that is specific for the truncated and constitutively active form of EGFR (EGFRvIII), which is only expressed in glioblastoma multiforme, was conjugated to iron oxide nanoparticle and imaged in murine models, after convection enhanced delivery (CED).[158] The targeted delivery of the antibody was also therapeutic since a significant decrease in glioblastoma cell survival was observed, alongside reduction in EGFR phosphorylation on immunohistochemical analysis of these cells.

A chemical biology approach can provide the ''tool-kit'' for combining different imaging modalities to examine tumours *in vivo*. For example, the matrix metalloproteinases (MMP) are involved in tumour invasion and metastasis. Fluorescent dendrimeric nanoparticles have been coated with activatable cell penetrating peptides (ACPPs) labelled with gadolinium, in order to bind to, and visualize MMPs by fluorescence imaging and MRI.[89] Active MMP-2 and MMP-9 on tumours were located in transgenic models, with fluorescence imaging and MRI. Fluorescent images detected post surgical residual tumour, and MRI was able to detect the spatial distribution of MMP within the tumour bulk. Often the tumours were surrounded by bright edges on MRI, tunnelling into normal tissue, thus visualizing the invasive and potentially metastatic process. Fluorescence imaging is limited in terms of depth of penetration, and clinically, is only validated for use with superficial disease *in vivo*. This technology is eminently applicable to the clinic for pre- or intra-operative resection, and assessing metastatic potential for primary tumours. For instance, a clinical application could involve direct visualisation of tumour cell migration to sentinel lymph nodes at surgery.

5.2 Linking whole body imaging to micro-/nanoscopic imaging of subcellular mechanisms on excised cancer tissues/cells

Whole body imaging of tumour pathophysiological processes such as hypoxia, angiogenesis, apoptosis and proliferation visualizes disease processes with millimetre resolution. In order to link these processes to molecular mechanisms which are mostly based on subcellular protein modifications (*e.g.* HER), such as dimerisation, phosphorylation and down-stream signal events must be visualized. One approach is to utilise whole body imaging modalities such as CT, PET, MRI or US to delineate disease at a whole body level and guide biopsy to specific sites of interest, where subcellular processes may be assessed by, *e.g.* FRET or optical imaging. This strategy represents complementary information that completes the description of the cancer molecular phenotype, when used with the *in vivo* methods described above, and the associated development of multiple tracers as imaging biomarkers.

Image-guided percutaneous biopsy is a well-established method in cancer diagnosis. For example, over the last 20 years, routine methods for the diagnosis and staging of breast cancer have relied on percutaneous biopsy under ultrasound or stereotactic mammographic guidance.[159] Breast cancer screening leads to a much higher detection rate of breast anomalies or microcalcifications. Most of these anomalies are not palpable and require image guidance to obtain diagnostic material. Image-guided biopsy has increased the accuracy of non-operative diagnosis and differentiation between malignant and benign disease from 63% to 95%. In the meantime patient morbidity has decreased due to a reduction in the rates of open surgical biopsy. Ultrasound-guided biopsy is also valuable in the neo-adjuvant setting in order to stage axillary lymph nodes for malignant infiltration. Fine-needle aspiration or core biopsies are taken and the tissue assessed for nuclear or histological grade, hormone receptor and HER2 status, in order to plan surgery, chemotherapy and targeted treatment. Newer methods of imaging in this setting include proton MRS of biopsy material, which has prognostic significance.[160] The chemical composition of cells may be measured from biopsy specimens with this method. However, 2D spectroscopy is also being applied *in vivo*, as an adjunct to MRI in order to delineate pathology in the whole breast at a subcellular level.[161] This technology is in its infancy but could help to highlight areas of interest for biopsy and to plan surgical intervention.

Another example of established image-guided biopsy techniques is the use of transrectal ultrasound (TRUS) as the gold standard method of visualising the prostate gland and determining potential malignant sites for biopsy.[162] However, up to 30% of cancers are missed at initial biopsy. A multiparametric MRI approach,[163] and co-registration of MRI and TRUS is being used to improve diagnosis and treatment, *e.g.* placement of brachytherapy beads. MRI has been used to guide transrectal and transperineal prostate biopsy, but procedural times are prolonged due to the added complication of a magnetic field, and thus procedural costs are high.[164] Co-registration of preprocedural MRI images and real-time TRUS solves these problems, and is potentially the most accurate method of image-guided biopsy for prostate

cancer.[165] The accuracy of TRUS–MRI fusion system is estimated to be 2.4 mm (±1.2 mm), which limits the detection size to lesions of 5 × 5 mm.[166]

These methods have been applied for initial cancer diagnosis and to plan surgery or radiotherapy. However, immunohistochemical information from the tissue obtained by image-guided

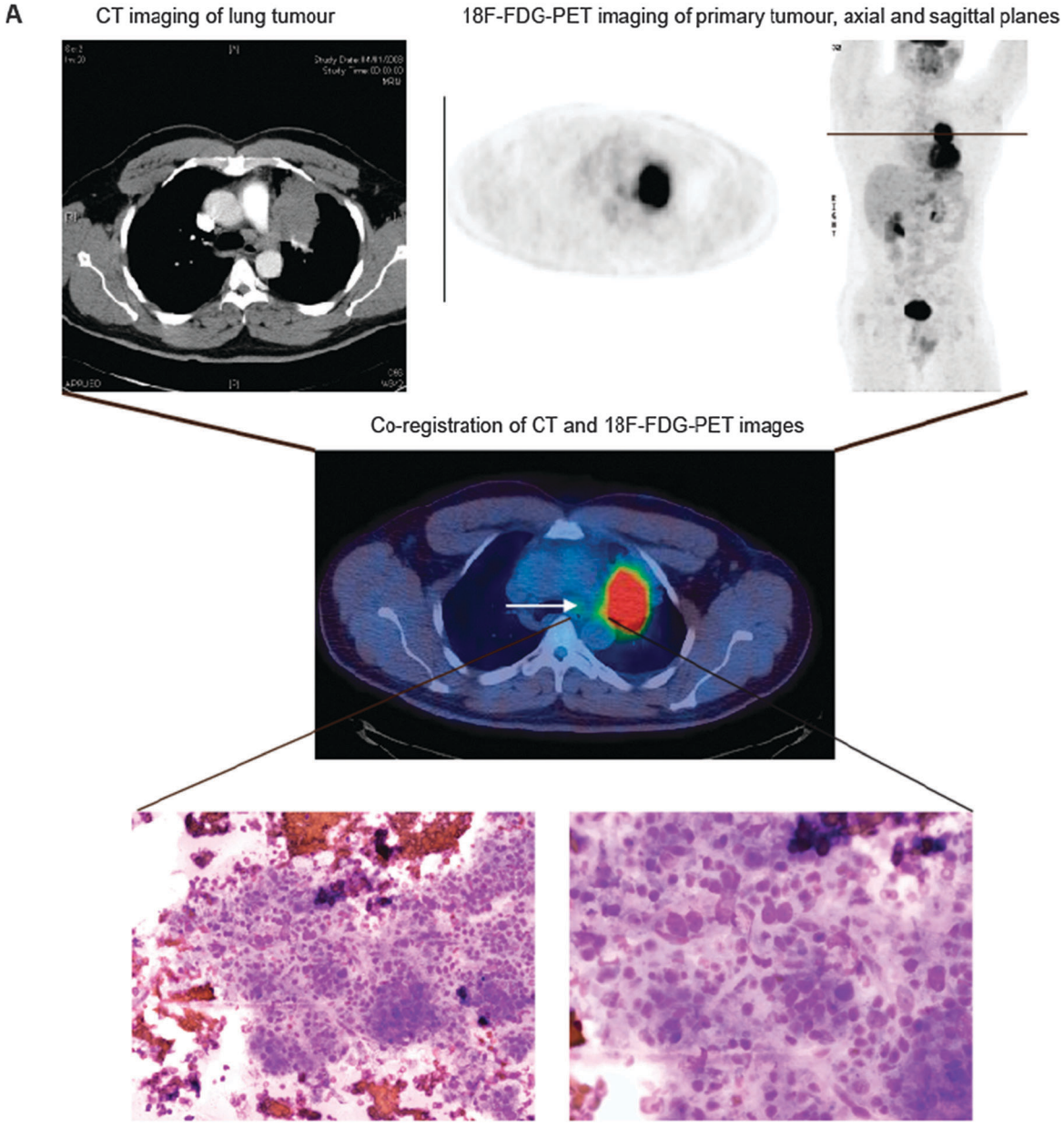

biopsy, may also be used to guide treatment decisions for chemotherapy and targeted therapy. For example, percutaneous ^{18}F-FDG-PET–CT guided bone biopsies have been shown to change the diagnostic staging, and thus alter planned treatment in over half of the cancer patients studied.[167] This group used repeated ^{18}F-FDG-PET–CT scans to position a needle in order to biopsy metabolically active bone lesions which were deemed equivocal on routine staging with CT, MRI or ^{18}F-FDG-PET.

Intended treatment was altered in 56% of patients (n = 20), with a variety of tumour types. For example, patients were treated with palliative rather than curative intent, or with systemic therapy rather than surgery. Included in this category were patients for whom the image-guided biopsies were investigated for hormone receptor or HER2 status by immunohistochemistry, which helped to decide on the appropriate treatment with anti-oestrogen drugs and/or trastuzumab. This study illustrates the benefits of the combination of two imaging modalities in order to correctly biopsy equivocal sites, which may impact on treatment decisions.

Using a similar principle, our group is developing a protocol in order to combine information from pre-procedural ^{18}F-FDG-PET scans with real time endobronchial ultrasound guided transbronchial fine needle aspiration (EBUS-TBNA) of mediastinal and hilar lymph nodes in non-small cell lung cancer (Fig. 1). Smears and cell block preparations of EBUS-TBNA aspirates can be screened for EGFR mutations that can render the tumour drug resistant, such as the T790M mutation which can confer gefitinib resistance; as well as for quantifying protein–protein interaction of interest, *e.g.* EGFR ubiquitination or EGFR heterodimerisation with HER2 (which has been shown to prevent EGFR dephosphorylation and signal termination by endomembrane-bound protein tyrosine phosphatases (PTPs)[169]) by fluorescence lifetime imaging (FLIM)/Förster resonance energy transfer (FRET) assays (see the following section). Subcellular imaging may be used to examine potential differences in these signalling events, at sites which are positive and negative on imaging with ^{18}F-FDG-PET. The success of treatment strategies may then be monitored (both spatially and temporally) by the changes in specific tumour cell mechanisms. In the future, molecular imaging may be carried out on image-guided biopsy material, in order to apply the right treatment regimen to the right patient at the right time. The main challenge to this strategy would be the difficulty in choosing the site for biopsy and the need to minimise multiple biopsies, and hence the need to improve the accuracy of currently available image-guidance techniques.

5.3 Subcellular imaging of pathological mechanisms—preclinical applications

Optical imaging, fluorescence and bioluminescence studies best describe subcellular protein–protein interactions and/or protein modifications such as phosphorylation, at a high spatial resolution. For instance, Förster resonance energy transfer (FRET) imaging by fluorescence lifetime imaging (FLIM) has been used to quantify protein–protein interactions at the nanometre scale, *in vitro* and in live cells/animals.[27–29,170,171] This technique measures energy transfer from an excited donor fluorophore to an acceptor molecule in close proximity. In order for FRET to occur, molecules must be within nanometre proximity.[172] Therefore this technique may be used to visualise protein–protein interactions or protein modifications within cells. FRET–FLIM technology can be used to interrogate the malignant proteome, and its response to treatment, thus providing a functional insight which was previously the mainstay of analytical biochemistry. An example of application of FRET technology is the development of the so-called 'Picchu' (phosphorylation indicator of the CrkII chimeric unit) FRET probe which can be used to monitor EGFR activity in preclinical models.[170] Preclinical experiments using this FRET sensor demonstrated that the EGFR receptor remains active after endocytosis, until translocation to the perinuclear region. This effect may be modulated by its ligand, epidermal growth factor (EGF) and by TKIs.

Another example of using FRET imaging to monitor, in the preclinical setting, the pharmacodynamic response to therapy *in situ* is the application of the probe SCAT3 to monitor caspase-3 activity during tumour cell apoptosis subsequent to cisplatin or photodynamic (PDT) treatment.[90] This technique was repeated at varying time-points in order to observe drug effects on the tumour. Such an assessment of 'on-target' drug effects could greatly improve response assessment. However, currently FRET quantification is limited to superficial tumours. Development of instruments combining endoscopic cellular resolution imaging with technology to quantify fluorescent lifetime and FRET, is underway and will increase potential clinical applications.[173]

Fig. 1 Endobronchial ultrasound guided transbronchial fine needle aspiration (EBUS-TBNA) to biopsy mediastinal lymph nodes in NSCLC. (A) Co-registration of images from CT and ^{18}F-FDG-PET combines spatial resolution of CT with the functional capacity of PET in order to stage this patient with non-small cell lung cancer. The middle image shows FDG uptake in the left upper lobe primary tumour (red spot) and very low FDG uptake in an adjacent left paratracheal lymph node, as demonstrated by the white arrow. The low FDG uptake in left paratracheal lymph node was not deemed to be significant but EBUS-guided transbronchial needle aspiration (TBNA) showed evidence of metastatic infiltration by non-small cell lung cancer (NSCLC). The H&E images (haematoxylin and eosin) show a mixed population of lymphocytes, but with a few groups of atypical cells. Within these cells, a high nuclear to cytoplasmic ratio, angulated and prominent nucleoli suggest malignant transformation. (B) FRET/FLIM assays are performed on samples obtained by EBUS-TBNA. EGFR ubiquitination is assessed by measuring FRET between anti-EGFR-Cy2 IgG and anti-ubiquitin-Cy3 IgG. Interaction between Cy2 and Cy3 results in a shortening of the lifetime of Cy2, as seen in the pseudocolour lifetime image. FRET efficiency was calculated using the following equation in each pixel and averaged per each cell. FRET efficiency = $1 - \tau_{da}/\tau_{control}$, where τ_{da} is the lifetime of cells stained with both anti-EGFR-Cy2 IgG and anti-ubiquitin-Cy3 IgG and $\tau_{control}$ is the mean anti-EGFR-Cy2 lifetime measured in the absence of acceptor. The lifetime error image on the far right illustrates the small error margins associated with this approach. Analysis was done using Bayesian fitting methods.[168] White scale bar represents 5 microns.

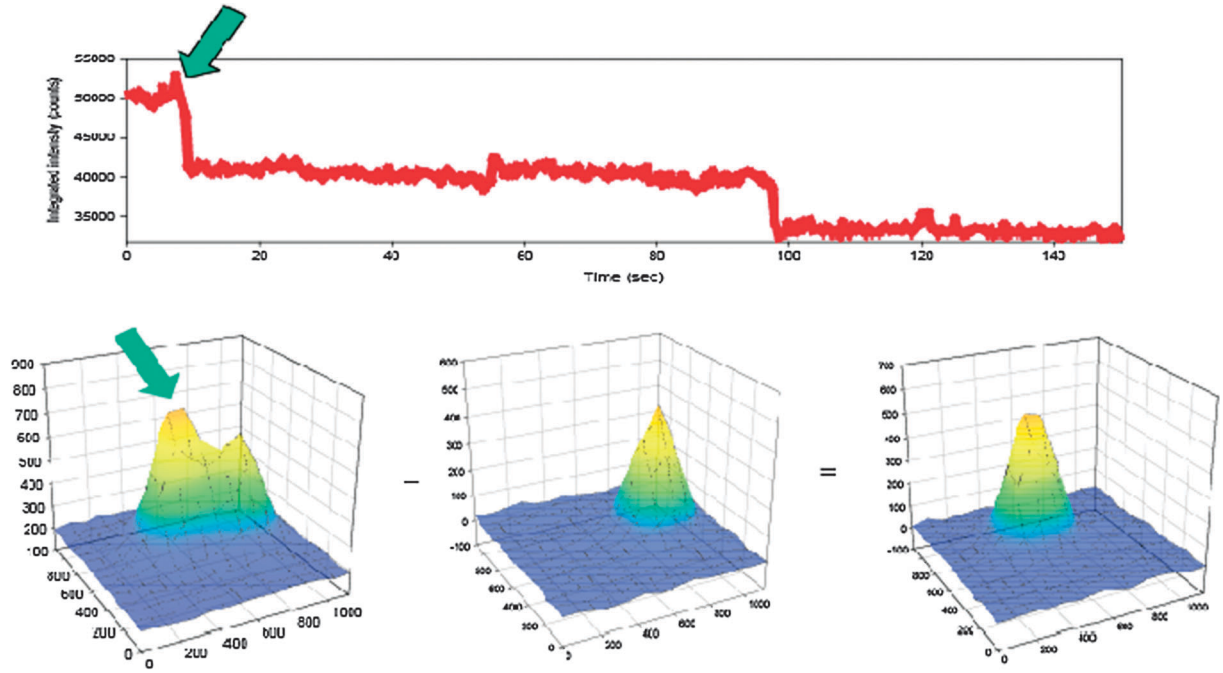

Fig. 2 Photobleaching as a method of colocalisation with SHRImP (single-molecule high resolution imaging with photobleaching) based upon fluorescence imaging with one nanometre accuracy (FIONA). SHRImP techniques measure the distance between two dyes which are closer than the diffraction-limit. In the case shown, the dyes can just be resolved; by conventional microscopy, they are 330 nm apart, fit by two Gaussians. In order to determine this distance by SHRImP, the sample is illuminated with light. Initially, fluorophores, for example, fluorophore F_1 and fluorophore F_2, are bright, in total emitting with 2 units of intensity as shown on the graph in the lower panel (far left). Over time one of the fluorophores (*e.g.* F_2) photobleaches, the intensity decreases to approximately 1 unit, and one of the Gaussian "hills" disappears, as shown in the middle graph. The position of the fluorophore which is still emitting, F_1, can be determined to a few nanometres by fitting the centroid of the "hill". The position of F_1 can then be calculated by subtracting the image of both emitting—$F_1 + F_2$—minus the emission after the photobleaching-F_2, and fitting the centroid, as shown in the graph on the far right. The difference in the two centroids, *i.e.* 326 nm, is the resolution. This has shown to be effective down to 10 nm between two dyes.[179]

Although FRET probes may be able to quantify direct protein–protein interactions, within 5–10 nm proximity, the spatial organisation of signalling proteins may be over the 10–250 nm scale on endosomal structures (including early endosomes to sorting endosomes and multivesicular bodies (MVBs)[174]). At this length scale, it may be difficult to quantify, using FRET imaging, the inter-receptor distance within homo-oligomers of EGFR,[175] and its heterodimer with other signalling receptors such as the c-Met receptor tyrosine kinase.[176,177] The spatial organisation of these receptors may provide significant insight into various mechanisms of resistance, for example anti-EGFR treatment by the acquisition of MET gene amplification.[178] In order to address this issue, a novel technique, is being applied, to map the 3D position of quantum-dot(QD)-labelled receptors in fixed breast cancer cells, within 3 nm accuracy, as shown in Fig. 2.

Modern super-resolution techniques can resolve the distance between identical molecules to about 8–10 nm; a significant improvement upon the conventional limit of resolution in visible microscopy, 200–250 nm. Two of the techniques are termed SHRImP (single-molecule high resolution imaging with photobleaching) or SHREC (single-molecule high-resolution colocalization). These techniques are both based on FIONA (fluorescence imaging with one nanometre accuracy), which is able to localise a single fluorophore within 1 nm accuracy. Despite the small size of the fluorophore (a few nanometres in width), its position is limited by diffraction which is approximately 250 nm. This is termed an airy function, and can be approximated by a Gaussian function, as shown in the lower panel of Fig. 2. Recent advances in detectors allow detection of the signal from an individual molecule so that the centroid of the Gaussian function can be located to 1 nm accuracy.

SHRImP and SHREC utilize FIONA to detect the difference between two nearby Gaussian functions. In the case of SHREC, one chooses two dyes whose emission spectra are well separated from each other. Using an appropriate filter set, one can individually detect the location of each dye to FIONA-type accuracy. The difference in the centroids is the resolution.[180] In SHRImP, the two dyes are exactly the same, and one relies on one of the identical dyes being turned off, generally by random photobleaching. The dye which is still emitting is located by FIONA to about one nanometre. The location of the original dye is obtained by subtraction of the emission immediately after photobleaching, from the image just before photobleaching. The resolution is then the difference of the position of the two centroids (Fig. 2). This procedure has been shown to work for molecules separated by 10–20 nm.[179] The SHRImP has been generalized to resolve distances among tens of molecules and achieve super-resolution imaging. Delineation of the spatial organisation

of receptors at the subcellular level may help describe the tumour molecular phenotype for selection of appropriate therapeutic agents.

5.4 Subcellular imaging of pathological mechanisms—clinical applications

We have established FRET–FLIM assays in cell line models of cancer, fresh human tissues and formalin-fixed paraffin-embedded tissue (FFPE), as well as dynamic deep tissue imaging of cancer cells in murine models.[28] Fig. 3 demonstrates the translation of an *in vitro* protein–protein assay, measuring EGFR ubiquitination, in cell lines, to a dual antibody-based assay for quantification of EGFR ubiquitination in tissue, using FRET/FLIM technology. These images demonstrate *in vitro* assessment of functional EGFR modifications, *i.e.* ubiquitination, which is associated with downregulation and degradation of this receptor.[129,181] Cell lines with varying susceptibility to EGFR degradation (panel B), mimic varying tumour phenotypes. Thus, translation of these assays for use in patient tumour tissue may delineate a group of patients who are more likely to respond to drugs manipulating this pathway.

Besides whole tumour sections or image-guided biopsy material (Fig. 1), clinically these FRET–FLIM assays could also be applied to single metastatic cells, or the disseminating/circulating tumour cells (DTC/CTC), which confer a poor prognostic outcome in epithelial carcinomas, such as breast, lung and prostate.[182] The current validated methods for detection of DTCs rely on blood or bone sampling prior to immunocyto-chemical or molecular analysis.[183] Bone marrow involvement delineates the metastatic group more accurately in breast cancer patients, but bone marrow biopsy is invasive and the cells obtained are often not viable.[184] Circulating cancer tumour cells in the blood have been identified by a variety of immunological approaches, including identification of epithelium-specific antigens, *e.g.* cytoskeleton-associated cytokeratins, surface adhesion molecules, or growth factor receptors, and by molecular PCR-based techniques. The presence or absence of DTCs in the blood both before and after treatment has been shown to correlate with treatment response.[185,186] Furthermore, the presence or absence of radiological signs of disease progression can be combined with CTC counts in blood to improve the prediction of overall survival in metastatic breast cancer patients undergoing therapy.[186]

The presence of micrometastases in the form of DTCs may confer a poor prognosis as the cells may exhibit the same characteristics as cancer stem cells. They are resistant to therapy, disseminate and grow at alternative sites and express many of the same surface markers as cancer stem cells, *e.g.* CD44, cytokeratin 19, and EpCAM.[187,188]

Molecular signatures obtained from the analysis of CTCs have also highlighted certain markers which may predict tumour dormancy.[188] Tumour dormancy is a phenomenon by which tumour cells evade eradication to become active many years later. The immune system has been demonstrated to play an important role in both animal models and in patients. For example, T-cell activation is strongly correlated with overall survival in patients with colon cancer, independent of primary tumour size or nodal status.[189] Further research is being carried out in order to characterise the malignant phenotype of these cells. This information may then lead to clues as to how to target these resistant cells, and thus eradicate minimal residual disease. For example, DTCs in the bone marrow have been shown to overexpress urokinase-type plasminogen activator receptor and the extracellular matrix metalloproteinase inducer.[190] These targets are amenable to both imaging and for therapeutic potential. Imaging modalities which can monitor these cells *in vivo* would be of value to accurately gauge risk of relapse, and requirement for adjuvant treatment.

5.5 Signalling networks to identify optimal drug combinations

The response to treatment and the number of therapies required to eradicate a tumour has been mathematically modelled and integrated into signalling networks. These networks take into account biological tumour characteristics, such as the level of cell turnover, the rate of mutations, increased tumour size, and biological fitness for clonal expansion, as described mainly, by *in vitro* research.[191] Information derived from *in vivo* molecular imaging techniques could feed into these networks and greatly improve their capacity for prediction of treatment response and to design optimal drug combinations.

For example, a breast cancer patient who had kinome sequencing that revealed approximately 100 000 somatic point mutations would need 4–5 non-cross-resistant drugs to battle her cancer, according to this model.[192] Computational modelling has been used to create receptor tyrosine kinase co-activation networks to model the complex and dynamic interactions involved in chemoresistance.[193] Receptor co-activation describes the simultaneous activation of two or more receptor tyrosine kinases in order to maintain robust intracellular signalling in the face of perturbations. For example, resistance to trastuzumab may be conferred by the presence of a hetero-trimer of HER2, HER3 and insulin-like growth factor receptor (IGF-R).[194] Similarly, co-activation of c-Met and EGFR leads to resistance to EGFR-tyrsoine kinase inhibition by, *e.g.* gefitinib.[178] However, a combination strategy using inhibitors of c-Met, EGFR, and platelet-derived growth factor receptor (PDGFR) is successful in reducing cell viability compared to single-agent treatment, as multiple co-activators are targeted.[195] Although this is a viable approach to chemoresistance, such a cocktail of drugs is unlikely to be tolerated in patients. The attractiveness of such networks is the ability to identify fragile points downstream of the activators which may be specifically targeted to overcome resistance. Recently HER3 was identified as an example of a fragile node, as well as a co-activator, in animal models.[176] However, the challenge in translation of these models for clinical use lies in the paucity of signalling data in humans. Networks constructed thus far rely on *in vitro* or biochemical analysis of tumour tissue. *In vivo* subcellular imaging techniques are likely to be the next step in providing the data required to further annotate these network maps for clinical use.

Conversely, signalling networks developed *in vitro* have the potential to identify novel imaging biomarkers for resistance or response, in order to optimise the use of targeted treatments

(a more detailed description of this approach can be found in ref. 196). Table 1 illustrates a selection of the many and varied biomarkers which may enter the clinical arena to optimise cancer therapy. However, the question of which biomarker should be imaged for a particular patient remains unanswered.

For example, an EGFR-centred protein network has been constructed and probed using small interfering RNA (siRNA), in order to highlight protein–protein interactions which may contribute to resistance or sensitivity to cancer therapy.[33] Several proteins of interest were identified as potential

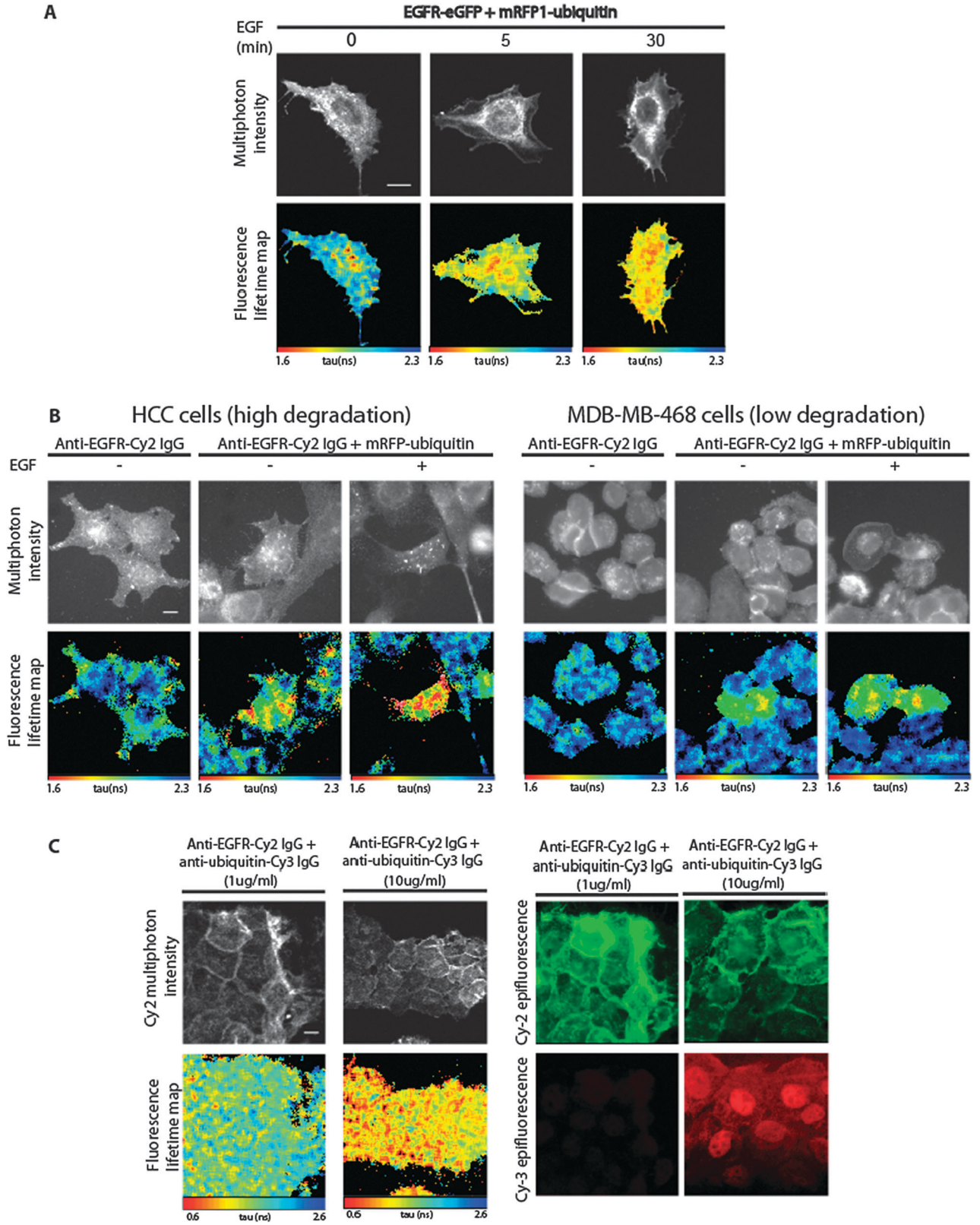

regulators of response to treatment and therefore, may be candidates for development as imaging biomarkers. However, the complexity and robustness of protein signalling networks combined with the intrinsic error rate associated with siRNA screens means that these potential targets require thorough validation *in vivo* prior to translation to the clinic.

In addition to application to signalling networks, clinical imaging modalities may provide prognostic information concurrent with established prognostic tools, such as gene expression signatures, in order to construct a mathematical model for outcome prediction. The development of microarray-based gene expression signatures has enabled classification of tumour subtypes and association with clinical outcome, notably in breast cancer.[19,197] A 70-gene prognostic signature for lymph node negative breast cancer patients is reported to provide prognostic information independent of clinicopathological scores and with improved sensitivity and specificity for poor clinical outcome.[198,199] A validation study of the 70-gene signature reported 90% sensitivity for metastasis within 5 years, for example, with specificity of 42%.[199] The tumour heterogeneity observed within intrinsic molecular subtypes of breast cancer is beginning to be described as deregulated molecular pathways at the gene expression level.[200] Clinical imaging traits have been used to partially reconstruct gene expression variation between tumours.[201] Association maps between clinical imaging features and gene expression variation have been constructed for CT image traits in hepatocellular carcinoma[202] and MRI traits in glioblastoma multiforme,[203] suggesting that imaging traits can approximately predict gene expression variation between tumours.

6. Conclusions

We have summarised a variety of potential applications for molecular imaging, ranging from the nanometre to the whole body scale, in the optimization of cancer therapy; *i.e.* choosing the right drug for the right patient at the right time. We have also discussed some of the challenges faced in the integration of molecular imaging into clinical practice.

Molecular imaging at a whole body level is unlikely to be possible using a single imaging modality. Tumour heterogeneity and a differential response to treatment represent a few of many characteristics influencing the eventual tumour phenotype, and thus, response to cancer therapeutics. Whole body imaging is the only technique currently available for the study of both primary tumour and metastases, both at diagnosis and to monitor response to treatment, but may not provide vital information at the molecular level. Image-guided biopsy, co-registration of complementary imaging modalities and appropriate biomarker choice may provide optimal risk stratification and help overcome these challenges. The issues of radiation dose and financial cost are yet to be fully addressed. Appropriate choice of imaging technology, the combination of modalities utilising ionising and non-ionising radiative sources and signal amplification may help alleviate some of the burden. Common quality assurance and control methods need to be developed in order to ensure a standard for imaging which may impact on treatment choice. This becomes increasingly difficult with rapidly evolving technology and whilst crossing national boundaries but is an area which requires future consideration.

Clinical outcome and response to treatment has a complex and multifaceted relationship to genotype and gene expression, dysregulation of signalling pathways *via* gene expression, protein activity, protein–protein interactions and tumour phenotypic traits. It may be possible to extract this data from patients using molecular imaging amongst other established techniques. However, the challenge is to integrate datasets from each observable level of variation, from genotype to tumour phenotype, in order to inform clinical management for the individual patient.

Acknowledgements

The authors would like to thank M. Keppler and A. Tutt for contributions to experimental work and for reviewing the manuscript, respectively. The authors acknowledge financial support from Cancer Research UK, the KCL–UCL Comprehensive Cancer Imaging Centre, funded by CR-UK & EPSRC, in association with the MRC and DoH, the National Institute for Health Research (NIHR) comprehensive Biomedical Research Centre, the Wellcome Trust, Guy's and St Thomas' Charity Foundation, Breakthrough Breast Cancer, the Experimental Cancer Medicine Centre Initiative (ECMC) in association with CR-UK, NIHR, Welsh Assembly Government, HSC R&D Office for Northern Ireland and Chief Scientist Office, Scotland and the National Institute for Health, General Medical Sciences.

Fig. 3 Multiphoton FLIM measurements of the intermolecular FRET between EGFR-eGFP and ubiquitin-mRFP1. A. MCF cells were transiently transfected with EGFR-eGFP in the presence or absence of mRFP1-ubiquitin to assess EGFR ubiquitination using a FRET-by-FLIM assay. Cells were either EGF treated (100 ng ml^{-1}, 30 min) or not. FRET between GFP and mRFP1 results in shortening of the fluorescence lifetime (τ) of GFP. FRET efficiency was calculated using the following equation in each pixel and averaged per each cell. FRET efficiency = $1 - \tau_{da}/\tau_{control}$, where τ_{da} is the fluorescence lifetime of cells co-expressing both EGFR-EGFP and mRFP1-ubiquitin and $\tau_{control}$ is the mean EGFR-EGFP lifetime measured in the absence of acceptor. B. Endogenous EGFR ubiquitination is assessed in the breast cancer cell lines, HCC and MDA-MB-468. EGFR ubiquitination is increased in cells which highly degrade EGFR on EGF treatment (HCC) as opposed to those which degrade EGFR less readily (MDA-MB-468). This is shown by the pseudocolour fluorescence lifetime maps. Here, FRET was measured between Cy2 and m-RFP. (C) Translation of the above FRET-by-FLIM assays to dual fluorophore-labelled antibody assays for application to endogenous protein interactions in tumour tissue. These Figures show the initial assessment of FRET efficiency between anti-EGFR-Cy2 and anti-ubiquitin-Cy3 in A431 cancer cells (with the established methodologies being applied to patient-derived cancer tissues). Anti-ubiquitin-Cy3 IgG concentration is at control level at 1ug ml^{-1}, whereby no ubiquitin staining is seen (epifluorescence Cy3 image), *versus* optimal concentration (10 ug ml^{-1}), whereby a reduction in fluorescence lifetime of Cy2 is seen on the pseudocolour lifetime images. White scale bars represent 5 microns.

Notes and references

1 J. A. DiMasi, R. W. Hansen and H. G. Grabowski, The price of innovation: new estimates of drug development costs, *J. Health Econ*., 2003, **22**, 151–85, DOI: 10.1016/S0167-6296(02)00126-1.

2 M. Fukuoka, S. Yano, G. Giaccone, T. Tamura, K. Nakagawa, J. Y. Douillard, Y. Nishiwaki, J. Vansteenkiste, S. Kudoh, D. Rischin, R. Eek, T. Horai, K. Noda, I. Takata, E. Smit, S. Averbuch, A. Macleod, A. Feyereislova, R. P. Dong and J. Baselga, Multi-institutional randomized phase II trial of gefitinib for previously treated patients with advanced non-small-cell lung cancer (The IDEAL 1 Trial) [corrected], *J. Clin. Oncol*., 2003, **21**, 2237–46; E. E. Cohen, F. Rosen, W. M. Stadler, W. Recant, K. Stenson, D. Huo and E. E. Vokes, Phase II trial of ZD1839 in recurrent or metastatic squamous cell carcinoma of the head and neck, *J. Clin. Oncol*., 2003, **21**, 1980–7; L. B. Saltz, N. J. Meropol, P. J. Loehrer, Sr., M. N. Needle, J. Kopit and R. J. Mayer, Phase II trial of cetuximab in patients with refractory colorectal cancer that expresses the epidermal growth factor receptor, *J. Clin. Oncol*., 2004, **22**, 1201–8; R. Perez-Soler, A. Chachoua, L. A. Hammond, E. K. Rowinsky, M. Huberman, D. Karp, J. Rigas, G. M. Clark, P. Santabarbara and P. Bonomi, Determinants of tumor response and survival with erlotinib in patients with non-small-cell lung cancer, *J. Clin. Oncol*., 2004, **22**, 3238–47.

3 L. Toschi and F. Cappuzzo, Understanding the new genetics of responsiveness to epidermal growth factor receptor tyrosine kinase inhibitors, *Oncologist*, 2007, **12**, 211–20, DOI: 10.1634/theoncologist.12-2-211.

4 F. Cappuzzo, V. Gregorc, E. Rossi, A. Cancellieri, E. Magrini, C. T. Paties, G. Ceresoli, L. Lombardo, S. Bartolini, C. Calandri, M. de Rosa, E. Villa and L. Crino, Gefitinib in pretreated non-small-cell lung cancer (NSCLC): analysis of efficacy and correlation with HER2 and epidermal growth factor receptor expression in locally advanced or metastatic NSCLC, *J. Clin. Oncol*., 2003, **21**, 2658–63, DOI: 10.1200/JCO.2003.01.039; H. S. Parra, R. Cavina, F. Latteri, P. A. Zucali, E. Campagnoli, E. Morenghi, G. C. Grimaldi, M. Roncalli and A. Santoro, Analysis of epidermal growth factor receptor expression as a predictive factor for response to gefitinib ('Iressa', ZD1839) in non-small-cell lung cancer, *Br. J. Cancer*, 2004, **91**, 208–12, DOI: 10.1038/sj.bjc.6601923.

5 J. G. Paez, P. A. Janne, J. C. Lee, S. Tracy, H. Greulich, S. Gabriel, P. Herman, F. J. Kaye, N. Lindeman, T. J. Boggon, K. Naoki, H. Sasaki, Y. Fujii, M. J. Eck, W. R. Sellers, B. E. Johnson and M. Meyerson, EGFR mutations in lung cancer: correlation with clinical response to gefitinib therapy, *Science*, 2004, **304**, 1497–500, DOI: 10.1126/science.1099314; T. J. Lynch, D. W. Bell, R. Sordella, S. Gurubhagavatula, R. A. Okimoto, B. W. Brannigan, P. L. Harris, S. M. Haserlat, J. G. Supko, F. G. Haluska, D. N. Louis, D. C. Christiani, J. Settleman and D. A. Haber, Activating mutations in the epidermal growth factor receptor underlying responsiveness of non-small-cell lung cancer to gefitinib, *N. Engl. J. Med*., 2004, **350**, 2129–39, DOI: 10.1056/NEJMoa040938.

6 Z. Chen, J. Feng, J. S. Saldivar, D. Gu, A. Bockholt and S. S. Sommer, EGFR somatic doublets in lung cancer are frequent and generally arise from a pair of driver mutations uncommonly seen as singlet mutations: one-third of doublets occur at five pairs of amino acids, *Oncogene*, 2008, **27**, 4336–43, DOI: 10.1038/onc.2008.71.

7 A. Hochhaus, S. Kreil, A. S. Corbin, P. La Rosee, M. C. Muller, T. Lahaye, B. Hanfstein, C. Schoch, N. C. Cross, U. Berger, H. Gschaidmeier, B. J. Druker and R. Hehlmann, Molecular and chromosomal mechanisms of resistance to imatinib (STI571) therapy, *Leukemia*, 2002, **16**, 2190–6, DOI: 10.1038/sj.leu.2402741.

8 M. W. Teng, J. B. Swann, C. M. Koebel, R. D. Schreiber and M. J. Smyth, Immune-mediated dormancy: an equilibrium with cancer, *J. Leukocyte Biol*., 2008, **84**, 988–93, DOI: 10.1189/jlb.1107774.

9 L. Fass, Imaging and cancer: a review, *Mol. Oncol*., 2008, **2**, 115–52, DOI: 10.1016/j.molonc.2008.04.001.

10 J. K. Willmann, N. van Bruggen, L. M. Dinkelborg and S. S. Gambhir, Molecular imaging in drug development, *Nat. Rev. Drug Discovery*, 2008, **7**, 591–607, DOI: 10.1038/nrd2290.

11 K. H. Bohuslavizki, Somatostatin receptor imaging: current status and future perspectives, *J. Nucl. Med*., 2001, **42**, 1057–8.

12 V. Ambrosini, D. Campana, P. Tomassetti, G. Grassetto, D. Rubello and S. Fanti, PET/CT with ^{68}Gallium-DOTA-peptides in NET: An overview, *Eur. J. Radiol*., 2010, DOI: 10.1016/j.ejrad.2010.07.022.

13 D. J. Kwekkeboom, B. L. Kam, M. van Essen, J. J. Teunissen, C. H. van Eijck, R. Valkema, M. de Jong, W. W. de Herder and E. P. Krenning, Somatostatin-receptor-based imaging and therapy of gastroenteropancreatic neuroendocrine tumors, *Endocr. Relat. Cancer*, 2009, **17**, R53–73, DOI: 10.1677/ERC-09-0078.

14 A. M. Groves, T. Win, S. B. Haim and P. J. Ell, Non-[^{18}F]FDG PET in clinical oncology, *Lancet Oncol*., 2007, **8**, 822–30, DOI: 10.1016/S1470-2045(07)70274-7.

15 G. Bertolini, L. Roz, P. Perego, M. Tortoreto, E. Fontanella, L. Gatti, G. Pratesi, A. Fabbri, F. Andriani, S. Tinelli, E. Roz, R. Caserini, S. Lo Vullo, T. Camerini, L. Mariani, D. Delia, E. Calabro, U. Pastorino and G. Sozzi, Highly tumorigenic lung cancer CD133+ cells display stem-like features and are spared by cisplatin treatment, *Proc. Natl. Acad. Sci. U. S. A*., 2009, **106**, 16281–6, DOI: 10.1073/pnas.0905653106.

16 S. Nimmagadda, M. Pullambhatla, K. Stone, G. Green, Z. M. Bhujwalla and M. G. Pomper, Molecular imaging of CXCR4 receptor expression in human cancer xenografts with [^{64}Cu]AMD3100 positron emission tomography, *Cancer Res*., 2010, **70**, 3935–44, DOI: 10.1158/0008-5472.CAN-09-4396.

17 T. F. Massoud and S. S. Gambhir, Molecular imaging in living subjects: seeing fundamental biological processes in a new light, *Genes Dev*., 2003, **17**, 545–80, DOI: 10.1101/gad.1047403.

18 U. Wilking, E. Karlsson, L. Skoog, T. Hatschek, E. Lidbrink, G. Elmberger, H. Johansson, L. Lindstrom and J. Bergh, HER2 status in a population-derived breast cancer cohort: discordances during tumor progression, *Breast Cancer Res. Treat*., 2010, **125**, 553, DOI: 10.1007/s10549-010-1029-2.

19 C. Sotiriou and L. Pusztai, Gene-expression signatures in breast cancer, *N. Engl. J. Med*., 2009, **360**, 790–800, DOI: 10.1056/NEJMra0801289.

20 D. C. Allred, Y. Wu, S. Mao, I. D. Nagtegaal, S. Lee, C. M. Perou, S. K. Mohsin, P. O'Connell, A. Tsimelzon and D. Medina, Ductal carcinoma *in situ* and the emergence of diversity during breast cancer evolution, *Clin. Cancer Res*., 2008, **14**, 370–8, DOI: 10.1158/1078-0432.CCR-07-1127; W. J. Lennington, R. A. Jensen, L. W. Dalton and D. L. Page, Ductal carcinoma *in situ* of the breast. Heterogeneity of individual lesions, *Cancer*, 1994, **73**, 118–24.

21 X. Chen, K. L. Reichenbach and C. Xu, Experimental and theoretical analysis of core-to-core coupling on fiber bundle imaging, *Opt. Express*, 2008, **16**, 21598–607, DOI: 10.1364/OE.16.021598; H. Inoue, S. E. Kudo and A. Shiokawa, Technology insight: Laser-scanning confocal microscopy and endocytoscopy for cellular observation of the gastrointestinal tract, *Nat. Clin. Pract. Gastroenterol. Hepatol*., 2005, **2**, 31–7, DOI: 10.1038/ncpgasthep0072.

22 J. Baselga and S. M. Swain, Novel anticancer targets: revisiting ERBB2 and discovering ERBB3, *Nat. Rev. Cancer*, 2009, **9**, 463–75, DOI: 10.1038/nrc2656.

23 H. Fan-Minogue, Z. Cao, R. Paulmurugan, C. T. Chan, T. F. Massoud, D. W. Felsher and S. S. Gambhir, Noninvasive molecular imaging of c-Myc activation in living mice, *Proc. Natl. Acad. Sci. U. S. A*., 2010, **107**, 15892, DOI: 10.1073/pnas.1007443107; A. De, P. Ray, A. M. Loening and S. S. Gambhir, BRET3: a red-shifted bioluminescence resonance energy transfer (BRET)-based integrated platform for imaging protein–protein interactions from single live cells and living animals, *FASEB J*., 2009, **23**, 2702–9, DOI: 10.1096/fj.08-118919.

24 T. F. Massoud, R. Paulmurugan and S. S. Gambhir, A molecularly engineered split reporter for imaging protein–protein interactions with positron emission tomography, *Nat. Med*., 2010, **16**, 921–6, DOI: 10.1038/nm.2185.

25 G. Tarcic, S. K. Boguslavsky, J. Wakim, T. Kiuchi, A. Liu, F. Reinitz, D. Nathanson, T. Takahashi, P. S. Mischel, T. Ng and Y. Yarden, An unbiased screen identifies DEP-1 tumor suppressor as a phosphatase controlling EGFR endocytosis, *Curr. Biol*., 2009, **19**, 1788–98; M. Parsons, J. Monypenny, S. M. Ameer-Beg, T. H. Millard, L. M. Machesky, M. Peter, M. D. Keppler, G. Schiavo, R. Watson, J. Chernoff, D. Zicha,

B. Vojnovic and T. Ng, Spatially distinct binding of Cdc42 to PAK1 and N-WASP in breast carcinoma cells, *Mol. Cell. Biol.*, 2005, **25**, 1680–95, DOI: 10.1128/MCB.25.5.1680-1695.2005; R. F. Carvalho, M. Beutler, K. J. Marler, B. Knoll, E. Becker-Barroso, R. Heintzmann, T. Ng and U. Drescher, Silencing of EphA3 through a cis interaction with ephrinA5, *Nat. Neurosci.*, 2006, **9**, 322–30; D. Romano, D. Matallanas, G. Weitsman, C. Preisinger, T. Ng and W. Kolch, Proapoptotic Kinase MST2 Coordinates Signaling Crosstalk between RASSF1A, Raf-1, and Akt, *Cancer Res.*, 2010, **70**, 1195–203; T. Ng, D. Shima, A. Squire, P. I. Bastiaens, S. Gschmeissner, M. J. Humphries and P. J. Parker, PKCalpha regulates beta1 integrin-dependent cell motility through association and control of integrin traffic, *EMBO J.*, 1999, **18**, 3909–23, DOI: 10.1093/emboj/18.14.3909; T. Niault, I. Sobczak, K. Meissl, G. E. Weitsman, D. Piazzolla, K. Ehrenreiter, M. Hamerl, I. Moarefi, T. Leung, O. Carugo, T. Ng and M. Baccarini, From Autoinhibition to Inhibition in Trans: the Raf-1 Regulatory Domain Inhibits Rok-a Kinase Activity, *J. Cell Biol.*, 2009, **187**, 335–342; N. Anilkumar, M. Parsons, R. Monk, T. Ng and J. C. Adams, Interaction of fascin and protein kinase Calpha: a novel intersection in cell adhesion and motility, *EMBO J.*, 2003, **22**, 5390–402, DOI: 10.1093/emboj/cdg521; K. Makrogianneli, L. M. Carlin, M. D. Keppler, D. R. Matthews, E. Ofo, A. Coolen, S. M. Ameer-Beg, P. R. Barber, B. Vojnovic and T. Ng, Integrating receptor signal inputs that influence small Rho GTPase activation dynamics at the immunological synapse, *Mol. Cell. Biol.*, 2009, **29**, 2997–3006; L. M. Carlin, K. Makrogianneli, M. Keppler, G. O. Fruhwirth and T. Ng, Visualisation of signalling in immune cells, *Methods Mol. Biol.*, 2010, **616**, 97–113, DOI: 10.1007/978-1-60761-461-6_7; D. R. Matthews, L. M. Carlin, E. Ofo, P. R. Barber, B. Vojnovic, M. Irving, T. Ng and S. M. Ameer-Beg, Time-lapse FRET microscopy using fluorescence anisotropy, *J. Microsc.*, 2010, **237**, 51–62, DOI: 10.1111/j.1365-2818.2009.03301.x; M. Beutler, K. Makrogianneli, R. J. Vermeij, M. Keppler, T. Ng, T. M. Jovin and R. Heintzmann, satFRET: estimation of Forster resonance energy transfer by acceptor saturation, *Eur. Biophys. J.*, 2008, **38**, 69–82, DOI: 10.1007/s00249-008-0361-5; S. J. Heasman, L. M. Carlin, S. Cox, T. Ng and A. J. Ridley, Coordinated RhoA signaling at the leading edge and uropod is required for T cell transendothelial migration, *J. Cell Biol.*, 2010, **190**, 553–63, DOI: 10.1083/jcb.201002067.

26 E. M. Bublil, G. Pines, G. Patel, G. Fruhwirth, T. Ng and Y. Yarden, Kinase-mediated quasi-dimers of EGFR, *FASEB J.*, 2010, **24**, 4744, DOI: 10.1096/fj.10-166199.

27 T. Ng, M. Parsons, W. E. Hughes, J. Monypenny, D. Zicha, A. Gautreau, M. Arpin, S. Gschmeissner, P. J. Verveer, P. I. Bastiaens and P. J. Parker, Ezrin is a downstream effector of trafficking PKC-integrin complexes involved in the control of cell motility, *EMBO J.*, 2001, **20**, 2723–41, DOI: 10.1093/emboj/20.11.2723; J. W. Legg, C. A. Lewis, M. Parsons, T. Ng and C. M. Isacke, A novel PKC-regulated mechanism controls CD44 ezrin association and directional cell motility, *Nat. Cell Biol.*, 2002, **4**, 399–407, DOI: 10.1038/ncb797.

28 M. T. Kelleher, G. Fruhwirth, G. Patel, E. Ofo, F. Festy, P. R. Barber, S. M. Ameer-Beg, B. Vojnovic, C. Gillett, A. Coolen, G. Keri, P. A. Ellis and T. Ng, The potential of optical proteomic technologies to individualize prognosis and guide rational treatment for cancer patients, *Targeted Oncol.*, 2009, **4**, 235–52, DOI: 10.1007/s11523-009-0116-y.

29 T. Ng, A. Squire, G. Hansra, F. Bornancin, C. Prevostel, A. Hanby, W. Harris, D. Barnes, S. Schmidt, H. Mellor, P. I. Bastiaens and P. J. Parker, Imaging protein kinase Calpha activation in cells, *Science*, 1999, **283**, 2085–9.

30 H. J. Choi, W. Ju, S. K. Myung and Y. Kim, Diagnostic performance of computer tomography, magnetic resonance imaging, and positron emission tomography or positron emission tomography/computer tomography for detection of metastatic lymph nodes in patients with cervical cancer: meta-analysis, *Cancer Sci.*, 2010, **101**, 1471–9, DOI: 10.1111/j.1349-7006.2010.01532.x; T. C. Kwee and R. M. Kwee, Combined FDG-PET/CT for the detection of unknown primary tumors: systematic review and meta-analysis, *Eur. Radiol.*, 2009, **19**, 731–44, DOI: 10.1007/s00330-008-1194-4.

31 L. Pan, P. Gu, G. Huang, H. Xue and S. Wu, Prognostic significance of SUV on PET/CT in patientswith esophageal cancer: a systematic review and meta-analysis, *Eur. J. Gastroenterol. Hepatol.*, 2009, **21**, 1008–15, DOI: 10.1097/MEG.0b013e328323d6fa; H. M. Quarles van Ufford, H. van Tinteren, S. G. Stroobants, Riphagen, II and O. S. Hoekstra, Added value of baseline ^{18}F-FDG uptake in serial ^{18}F-FDG PET for evaluation of response of solid extracerebral tumors to systemic cytotoxic neoadjuvant treatment: a meta-analysis, *J. Nucl. Med.*, 2010, **51**, 1507–16, DOI: 10.2967/jnumed.110.075457; L. S. Poulou, L. Thanos and P. D. Ziakas, Unifying the predictive value of pretransplant FDG PET in patients with lymphoma: a review and meta-analysis of published trials, *Eur. J. Nucl. Med. Mol. Imaging*, 2009, **37**, 156–62, DOI: 10.1007/s00259-009-1258-y.

32 M. Paesmans, T. Berghmans, M. Dusart, C. Garcia, C. Hossein-Foucher, J. J. Lafitte, C. Mascaux, A. P. Meert, M. Roelandts, A. Scherpereel, V. Terrones Munoz and J. P. Sculier, Primary tumor standardized uptake value measured on fluorodeoxyglucose positron emission tomography is of prognostic value for survival in non-small cell lung cancer: update of a systematic review and meta-analysis by the European Lung Cancer Working Party for the International Association for the Study of Lung Cancer Staging Project, *J. Thorac. Oncol.*, 2010, **5**, 612–9, DOI: 10.1097/JTO.0b013e3181d0a4f5.

33 I. Astsaturov, V. Ratushny, A. Sukhanova, M. B. Einarson, T. Bagnyukova, Y. Zhou, K. Devarajan, J. S. Silverman, N. Tikhmyanova, N. Skobeleva, A. Pecherskaya, R. E. Nasto, C. Sharma, S. A. Jablonski, I. G. Serebriiskii, L. M. Weiner and E. A. Golemis, Synthetic lethal screen of an EGFR-centered network to improve targeted therapies, *Sci. Signaling*, 2010, **3**, ra67, DOI: 10.1126/scisignal.2001083.

34 W. A. Weber, Use of PET for monitoring cancer therapy and for predicting outcome, *J. Nucl. Med.*, 2005, **46**, 983–95.

35 R. Boellaard, M. J. O'Doherty, W. A. Weber, F. M. Mottaghy, M. N. Lonsdale, S. G. Stroobants, W. J. Oyen, J. Kotzerke, O. S. Hoekstra, J. Pruim, P. K. Marsden, K. Tatsch, C. J. Hoekstra, E. P. Visser, B. Arends, F. J. Verzijlbergen, J. M. Zijlstra, E. F. Comans, A. A. Lammertsma, A. M. Paans, A. T. Willemsen, T. Beyer, A. Bockisch, C. Schaefer-Prokop, D. Delbeke, R. P. Baum, A. Chiti and B. J. Krause, FDG PET and PET/CT: EANM procedure guidelines for tumour PET imaging: version 1.0, *Eur. J. Nucl. Med. Mol. Imaging*, 2009, **37**, 181–200, DOI: 10.1007/s00259-009-1297-4.

36 A. Szafer, J. Zhong, A. W. Anderson and J. C. Gore, Diffusion-weighted imaging in tissues: theoretical models, *NMR Biomed.*, 1995, **8**, 289–96; C. H. Sotak, Nuclear magnetic resonance (NMR) measurement of the apparent diffusion coefficient (ADC) of tissue water and its relationship to cell volume changes in pathological states, *Neurochem. Int.*, 2004, **45**, 569–82, DOI: 10.1016/j.neuint.2003.11.010; A. R. Padhani, G. Liu, D. M. Koh, T. L. Chenevert, H. C. Thoeny, T. Takahara, A. Dzik-Jurasz, B. D. Ross, M. Van Cauteren, D. Collins, D. A. Hammoud, G. J. Rustin, B. Taouli and P. L. Choyke, Diffusion-weighted magnetic resonance imaging as a cancer biomarker: consensus and recommendations, *Neoplasia*, 2009, **11**, 102–25.

37 R. G. Kierkels, W. H. Backes, M. H. Janssen, J. Buijsen, R. G. Beets-Tan, P. Lambin, G. Lammering, M. C. Oellers and H. J. Aerts, Comparison between perfusion computed tomography and dynamic contrast-enhanced magnetic resonance imaging in rectal cancer, *Int. J. Radiat. Oncol., Biol., Phys.*, 2010, **77**, 400–8, DOI: 10.1016/j.ijrobp.2009.05.015; V. Goh, M. Dattani, J. Farwell, J. Shekhdar, E. Tam, S. Patel, J. Juttla, I. Simcock, J. Stirling, H. Mandeville, E. Aird and P. Hoskin, Radiation dose from volumetric helical perfusion CT of the thorax, abdomen or pelvis, *Eur. Radiol.*, 2010, **21**, 974, DOI: 10.1007/s00330-010-1997-y.

38 S. M. Eschmann, F. Paulsen, M. Reimold, H. Dittmann, S. Welz, G. Reischl, H. J. Machulla and R. Bares, Prognostic impact of hypoxia imaging with ^{18}F-misonidazole PET in non-small cell lung cancer and head and neck cancer before radiotherapy, *J. Nucl. Med.*, 2005, **46**, 253–60.

39 H. Schoder and M. Gonen, Screening for cancer with PET and PET/CT: potential and limitations, *J. Nucl. Med., Suppl.*, 2007, **48**(Suppl 1), 4S–18S.

40 M. E. Juweid and B. D. Cheson, Positron-emission tomography and assessment of cancer therapy, *N. Engl. J. Med.*, 2006, **354**, 496–507, DOI: 10.1056/NEJMra050276; P. Seam, M. E. Juweid and B. D. Cheson, The role of FDG-PET scans in patients with lymphoma, *Blood*, 2007, **110**, 3507–16, DOI: 10.1182/blood-2007-06-097238.
41 R. J. Downey, T. Akhurst, M. Gonen, A. Vincent, M. S. Bains, S. Larson and V. Rusch, Preoperative F-18 fluorodeoxyglucose-positron emission tomography maximal standardized uptake value predicts survival after lung cancer resection, *J. Clin. Oncol.*, 2004, **22**, 3255–60, DOI: 10.1200/JCO.2004.11.109.
42 K. A. Miles, Functional CT imaging in oncology, *Eur. J. Radiol.*, 2003, **13**(Suppl 5), M134–8.
43 Q. S. Ng, V. Goh, H. Fichte, E. Klotz, P. Fernie, M. I. Saunders, P. J. Hoskin and A. R. Padhani, Lung cancer perfusion at multi-detector row CT: reproducibility of whole tumor quantitative measurements, *Radiology*, 2006, **239**, 547–53, DOI: 10.1148/radiol.2392050568.
44 J. Yee, G. A. Akerkar, R. K. Hung, A. M. Steinauer-Gebauer, S. D. Wall and K. R. McQuaid, Colorectal neoplasia: performance characteristics of CT colonography for detection in 300 patients, *Radiology*, 2001, **219**, 685–92.
45 E. D. Pisano, C. Gatsonis, E. Hendrick, M. Yaffe, J. K. Baum, S. Acharyya, E. F. Conant, L. L. Fajardo, L. Bassett, C. D'Orsi, R. Jong and M. Rebner, Diagnostic performance of digital *versus* film mammography for breast-cancer screening, *N. Engl. J. Med.*, 2005, **353**, 1773–83, DOI: 10.1056/NEJMoa052911.
46 C. H. Holdsworth, R. D. Badawi, J. B. Manola, M. F. Kijewski, D. A. Israel, G. D. Demetri and A. D. Van den Abbeele, CT and PET: early prognostic indicators of response to imatinib mesylate in patients with gastrointestinal stromal tumor, *AJR, Am. J. Roentgenol.*, 2007, **189**, W324–30, DOI: 10.2214/AJR.07.2496; C. Y. Wong, J. Schmidt, J. S. Bong, S. Chundru, L. Kestin, D. Yan, I. Grills, M. Gaskill, V. Cheng, A. A. Martinez and D. Fink-Bennett, Correlating metabolic and anatomic responses of primary lung cancers to radiotherapy by combined F-18 FDG PET-CT imaging, *Radiat. Oncol.*, 2007, **2**, 18, DOI: 10.1186/1748-717X-2-18; H. Kato, M. Fukuchi, T. Miyazaki, M. Nakajima, N. Tanaka, T. Inose, H. Kimura, A. Faried, K. Saito, M. Sohda, Y. Fukai, N. Masuda, R. Manda, H. Ojima, K. Tsukada, N. Oriuchi, K. Endo, T. Nonaka, M. Shioya, H. Ishikawa, H. Sakurai, T. Nakano and H. Kuwano, Prediction of response to definitive chemoradiotherapy in esophageal cancer using positron emission tomography, *Anticancer Res.*, 2007, **27**, 2627–33.
47 L. F. de Geus-Oei, H. F. van der Heijden, E. P. Visser, R. Hermsen, B. A. van Hoorn, J. N. Timmer-Bonte, A. T. Willemsen, J. Pruim, F. H. Corstens, P. F. Krabbe and W. J. Oyen, Chemotherapy response evaluation with ^{18}F-FDG PET in patients with non-small cell lung cancer, *J. Nucl. Med.*, 2007, **48**, 1592–8, DOI: 10.2967/jnumed.107.043414.
48 L. F. de Geus-Oei, H. W. van Laarhoven, E. P. Visser, R. Hermsen, B. A. van Hoorn, Y. J. Kamm, P. F. Krabbe, F. H. Corstens, C. J. Punt and W. J. Oyen, Chemotherapy response evaluation with FDG-PET in patients with colorectal cancer, *Ann. Oncol.*, 2008, **19**, 348–52, DOI: 10.1093/annonc/mdm470.
49 N. Rizk, R. J. Downey, T. Akhurst, M. Gonen, M. S. Bains, S. Larson and V. Rusch, Preoperative 18[F]-fluorodeoxyglucose positron emission tomography standardized uptake values predict survival after esophageal adenocarcinoma resection, *Ann. Thorac. Surg.*, 2006, **81**, 1076–81, DOI: 10.1016/j.athoracsur.2005.09.063; R. J. Robbins, Q. Wan, R. K. Grewal, R. Reibke, M. Gonen, H. W. Strauss, R. M. Tuttle, W. Drucker and S. M. Larson, Real-time prognosis for metastatic thyroid carcinoma based on 2-[^{18}F]fluoro-2-deoxy-D-glucose-positron emission tomography scanning, *J. Clin. Endocrinol. Metab.*, 2006, **91**, 498–505, DOI: 10.1210/jc.2005-1534.
50 S. C. Huang, Anatomy of SUV. Standardized uptake value, *Nucl. Med. Biol.*, 2000, **27**, 643–6, DOI: 10.1016/S0969-8051(00)00155-4.
51 W. A. Berg, I. N. Weinberg, D. Narayanan, M. E. Lobrano, E. Ross, L. Amodei, L. Tafra, L. P. Adler, J. Uddo, W. Stein, 3rd and E. A. Levine, High-resolution fluorodeoxyglucose positron emission tomography with compression ("positron emission mammography") is highly accurate in depicting primary breast cancer, *Breast J.*, 2006, **12**, 309–23, DOI: 10.1111/j.1075-122X.2006.00269.x.
52 M. Souvatzoglou, A. L. Grosu, B. Roper, B. J. Krause, R. Beck, G. Reischl, M. Picchio, H. J. Machulla, H. J. Wester and M. Piert, Tumour hypoxia imaging with [^{18}F]FAZA PET in head and neck cancer patients: a pilot study, *Eur. J. Nucl. Med. Mol. Imaging*, 2007, **34**, 1566–75, DOI: 10.1007/s00259-007-0424-3.
53 L. Kenny, R. C. Coombes, D. M. Vigushin, A. Al-Nahhas, S. Shousha and E. O. Aboagye, Imaging early changes in proliferation at 1 week post chemotherapy: a pilot study in breast cancer patients with 3′-deoxy-3′-[^{18}F]fluorothymidine positron emission tomography, *Eur. J. Nucl. Med. Mol. Imaging*, 2007, **34**, 1339–47, DOI: 10.1007/s00259-007-0379-4; Y. J. Yang, J. S. Ryu, S. Y. Kim, S. J. Oh, K. C. Im, H. Lee, S. W. Lee, K. J. Cho, G. J. Cheon and D. H. Moon, Use of 3′-deoxy-3′-[^{18}F]fluorothymidine PET to monitor early responses to radiation therapy in murine SCCVII tumors, *Eur. J. Nucl. Med. Mol. Imaging*, 2006, **33**, 412–9, DOI: 10.1007/s00259-005-0011-4.
54 K. J. Yagle, J. F. Eary, J. F. Tait, J. R. Grierson, J. M. Link, B. Lewellen, D. F. Gibson and K. A. Krohn, Evaluation of ^{18}F-annexin V as a PET imaging agent in an animal model of apoptosis, *J. Nucl. Med.*, 2005, **46**, 658–66.
55 H. M. Linden, S. A. Stekhova, J. M. Link, J. R. Gralow, R. B. Livingston, G. K. Ellis, P. H. Petra, L. M. Peterson, E. K. Schubert, L. K. Dunnwald, K. A. Krohn and D. A. Mankoff, Quantitative fluoroestradiol positron emission tomography imaging predicts response to endocrine treatment in breast cancer, *J. Clin. Oncol.*, 2006, **24**, 2793–9, DOI: 10.1200/JCO.2005.04.3810.
56 C. L. Ho, S. C. Yu and D. W. Yeung, ^{11}C-acetate PET imaging in hepatocellular carcinoma and other liver masses, *J. Nucl. Med.*, 2003, **44**, 213–21; T. Ohtani, H. Kurihara, S. Ishiuchi, N. Saito, N. Oriuchi, T. Inoue and T. Sasaki, Brain tumour imaging with carbon-11 choline: comparison with FDG PET and gadolinium-enhanced MR imaging, *Eur. J. Nucl. Med. Mol. Imaging*, 2001, **28**, 1664–70, DOI: 10.1007/s002590100620.
57 M. K. Robinson, M. Doss, C. Shaller, D. Narayanan, J. D. Marks, L. P. Adler, D. E. Gonzalez Trotter and G. P. Adams, Quantitative immuno-positron emission tomography imaging of HER2-positive tumor xenografts with an iodine-124 labeled anti-HER2 diabody, *Cancer Res.*, 2005, **65**, 1471–8, DOI: 10.1158/0008-5472.CAN-04-2008.
58 P. K. Borjesson, Y. W. Jauw, R. de Bree, J. C. Roos, J. A. Castelijns, C. R. Leemans, G. A. van Dongen and R. Boellaard, Radiation dosimetry of ^{89}Zr-labeled chimeric monoclonal antibody U36 as used for immuno-PET in head and neck cancer patients, *J. Nucl. Med.*, 2009, **50**, 1828–36, DOI: 10.2967/jnumed.109.065862.
59 X. Zhang, Z. Xiong, Y. Wu, W. Cai, J. R. Tseng, S. S. Gambhir and X. Chen, Quantitative PET imaging of tumor integrin $\alpha\beta3$ expression with ^{18}F-FRGD2, *J. Nucl. Med.*, 2006, **47**, 113–21.
60 P. M. Smith-Jones, D. B. Solit, T. Akhurst, F. Afroze, N. Rosen and S. M. Larson, Imaging the pharmacodynamics of HER2 degradation in response to Hsp90 inhibitors, *Nat. Biotechnol.*, 2004, **22**, 701–6, DOI: 10.1038/nbt968; D. B. Solit, S. P. Ivy, C. Kopil, R. Sikorski, M. J. Morris, S. F. Slovin, W. K. Kelly, A. DeLaCruz, T. Curley, G. Heller, S. Larson, L. Schwartz, M. J. Egorin, N. Rosen and H. I. Scher, Phase I trial of 17-allylamino-17-demethoxygeldanamycin in patients with advanced cancer, *Clin. Cancer Res.*, 2007, **13**, 1775–82, DOI: 10.1158/1078-0432.CCR-06-1863; P. M. Smith-Jones, D. Solit, F. Afroze, N. Rosen and S. M. Larson, Early tumor response to Hsp90 therapy using HER2 PET: comparison with ^{18}F-FDG PET, *J. Nucl. Med.*, 2006, **47**, 793–6.
61 M. V. Backer, Z. Levashova, V. Patel, B. T. Jehning, K. Claffey, F. G. Blankenberg and J. M. Backer, Molecular imaging of VEGF receptors in angiogenic vasculature with single-chain VEGF-based probes, *Nat. Med.*, 2007, **13**, 504–9, DOI: 10.1038/nm1522.
62 K. A. Kurdziel, D. O. Kiesewetter, R. E. Carson, W. C. Eckelman and P. Herscovitch, Biodistribution, radiation dose estimates, and *in vivo* Pgp modulation studies of ^{18}F-paclitaxel in nonhuman primates, *J. Nucl. Med.*, 2003, **44**, 1330–9; T. Inoue, E. E. Kim, S. Wallace, D. J. Yang, F. C. Wong, P. Bassa, A. Cherif, E. Delpassand, A. Buzdar and D. A. Podoloff, Positron emission tomography using [^{18}F]fluorotamoxifen to evaluate therapeutic responses in patients with breast cancer: preliminary study,

Cancer Biother. Radiopharm., 1996, **11**, 235–45; M. Moehler, A. Dimitrakopoulou-Strauss, F. Gutzler, U. Raeth, L. G. Strauss and W. Stremmel, ^{18}F-labeled fluorouracil positron emission tomography and the prognoses of colorectal carcinoma patients with metastases to the liver treated with 5-fluorouracil, *Cancer*, 1998, **83**, 245–53, DOI: 10.1002/(SICI)1097-0142(19980715)83:2<245::AID-CNCR7>3.0.CO;2-P; J. Z. Ginos, A. J. Cooper, V. Dhawan, J. C. Lai, S. C. Strother, N. Alcock and D. A. Rottenberg, [^{13}N]cisplatin PET to assess pharmacokinetics of intra-arterial *versus* intravenous chemotherapy for malignant brain tumors, *J. Nucl. Med.*, 1987, **28**, 1844–52.

63 S. M. Larson and H. Schoder, New PET tracers for evaluation of solid tumor response to therapy, *Q. J. Nucl. Med. Mol. Imaging*, 2009, **53**, 158–66.

64 M. Bhattacharyya, D. Ryan, R. Carpenter, S. Vinnicombe and C. J. Gallagher, Using MRI to plan breast-conserving surgery following neoadjuvant chemotherapy for early breast cancer, *Br. J. Cancer*, 2008, **98**, 289–93, DOI: 10.1038/sj.bjc.6604171.

65 E. Warner, H. Messersmith, P. Causer, A. Eisen, R. Shumak and D. Plewes, Systematic review: using magnetic resonance imaging to screen women at high risk for breast cancer, *Ann. Intern. Med.*, 2008, **148**, 671–9; M. O. Leach, MRI for breast cancer screening, *Ann. Oncol.*, 2006, **17**(Suppl 10), x325–31, DOI: 10.1093/annonc/mdl281.

66 A. R. Padhani, C. Hayes, L. Assersohn, T. Powles, A. Makris, J. Suckling, M. O. Leach and J. E. Husband, Prediction of clinicopathologic response of breast cancer to primary chemotherapy at contrast-enhanced MR imaging: initial clinical results, *Radiology*, 2006, **239**, 361–74, DOI: 10.1148/radiol.2392021099.

67 M. L. George, A. S. Dzik-Jurasz, A. R. Padhani, G. Brown, D. M. Tait, S. A. Eccles and R. I. Swift, Non-invasive methods of assessing angiogenesis and their value in predicting response to treatment in colorectal cancer, *Br. J. Surg.*, 2001, **88**, 1628–36, DOI: 10.1046/j.0007-1323.2001.01947.x.

68 M. O. Leach, K. M. Brindle, J. L. Evelhoch, J. R. Griffiths, M. R. Horsman, A. Jackson, G. C. Jayson, I. R. Judson, M. V. Knopp, R. J. Maxwell, D. McIntyre, A. R. Padhani, P. Price, R. Rathbone, G. J. Rustin, P. S. Tofts, G. M. Tozer, W. Vennart, J. C. Waterton, S. R. Williams and P. Workman, The assessment of antiangiogenic and antivascular therapies in early-stage clinical trials using magnetic resonance imaging: issues and recommendations, *Br. J. Cancer*, 2005, **92**, 1599–610, DOI: 10.1038/sj.bjc.6602550.

69 K. M. Brindle, Molecular imaging using magnetic resonance: new tools for the development of tumour therapy, *Br. J. Radiol.*, 2003, **76**(Spec. No. 2), S111–7; P. M. Winter, S. D. Caruthers, A. Kassner, T. D. Harris, L. K. Chinen, J. S. Allen, E. K. Lacy, H. Zhang, J. D. Robertson, S. A. Wickline and G. M. Lanza, Molecular imaging of angiogenesis in nascent Vx-2 rabbit tumors using a novel $\alpha(v)\beta3$-targeted nanoparticle and 1.5 tesla magnetic resonance imaging, *Cancer Res.*, 2003, **63**, 5838–43.

70 P. M. Winter, A. H. Schmieder, S. D. Caruthers, J. L. Keene, H. Zhang, S. A. Wickline and G. M. Lanza, Minute dosages of alpha(nu)beta3-targeted fumagillin nanoparticles impair Vx-2 tumor angiogenesis and development in rabbits, *FASEB J.*, 2008, **22**, 2758–67, DOI: 10.1096/fj.07-103929.

71 T. W. Stadnik, H. Everaert, S. Makkat, R. Sacre, J. Lamote and C. Bourgain, Breast imaging. Preoperative breast cancer staging: comparison of USPIO-enhanced MR imaging and ^{18}F-fluorodeoxyglucose (FDC) positron emission tomography (PET) imaging for axillary lymph node staging-initial findings, *Eur. Radiol.*, 2006, **16**, 2153–60, DOI: 10.1007/s00330-006-0276-4.

72 W. M. Deserno, M. G. Harisinghani, M. Taupitz, G. J. Jager, J. A. Witjes, P. F. Mulders, C. A. Hulsbergen van de Kaa, D. Kaufmann and J. O. Barentsz, Urinary bladder cancer: preoperative nodal staging with ferumoxtran-10-enhanced MR imaging, *Radiology*, 2004, **233**, 449–56, DOI: 10.1148/radiol.2332031111; M. G. Harisinghani, J. Barentsz, P. F. Hahn, W. M. Deserno, S. Tabatabaei, C. H. van de Kaa, J. de la Rosette and R. Weissleder, Noninvasive detection of clinically occult lymph-node metastases in prostate cancer, *N. Engl. J. Med.*, 2003, **348**, 2491–9, DOI: 10.1056/NEJMoa022749.

73 M. Zhao, D. A. Beauregard, L. Loizou, B. Davletov and K. M. Brindle, Non-invasive detection of apoptosis using magnetic resonance imaging and a targeted contrast agent, *Nat. Med.*, 2001, **7**, 1241–4, DOI: 10.1038/nm1101-1241.

74 D. Artemov, N. Mori, B. Okollie and Z. M. Bhujwalla, MR molecular imaging of the Her-2/neu receptor in breast cancer cells using targeted iron oxide nanoparticles, *Magn. Reson. Med.*, 2003, **49**, 403–8, DOI: 10.1002/mrm.10406.

75 W. J. Rogers, C. H. Meyer and C. M. Kramer, Technology insight: *in vivo* cell tracking by use of MRI, *Nat. Clin. Pract. Cardiovasc. Med.*, 2006, **3**, 554–62, DOI: 10.1038/ncpcardio0659.

76 E. A. Schellenberger, D. Hogemann, L. Josephson and R. Weissleder, Annexin V-CLIO: a nanoparticle for detecting apoptosis by MRI, *Acad. Radiol.*, 2002, **9**(Suppl 2), S310–1.

77 D. Le Bihan, C. Poupon, A. Amadon and F. Lethimonnier, Artifacts and pitfalls in diffusion MRI, *J. Magn. Reson. Imaging*, 2006, **24**, 478–88, DOI: 10.1002/jmri.20683.

78 D. A. Hamstra, T. L. Chenevert, B. A. Moffat, T. D. Johnson, C. R. Meyer, S. K. Mukherji, D. J. Quint, S. S. Gebarski, X. Fan, C. I. Tsien, T. S. Lawrence, L. Junck, A. Rehemtulla and B. D. Ross, Evaluation of the functional diffusion map as an early biomarker of time-to-progression and overall survival in high-grade glioma, *Proc. Natl. Acad. Sci. U. S. A.*, 2005, **102**, 16759–64, DOI: 10.1073/pnas.0508347102.

79 M. D. Pickles, P. Gibbs, M. Lowry and L. W. Turnbull, Diffusion changes precede size reduction in neoadjuvant treatment of breast cancer, *Magn. Reson. Imaging*, 2006, **24**, 843–7, DOI: 10.1016/j.mri.2005.11.005.

80 E. J. Vlieger, C. B. Majoie, S. Leenstra and G. J. Den Heeten, Functional magnetic resonance imaging for neurosurgical planning in neurooncology, *Eur. Radiol.*, 2004, **14**, 1143–53, DOI: 10.1007/s00330-004-2328-y.

81 S. P. Li, N. J. Taylor, A. Makris, M. L. Ah-See, M. J. Beresford, J. J. Stirling, J. A. d'Arcy, D. J. Collins and A. R. Padhani, Primary Human Breast Adenocarcinoma: Imaging and Histologic Correlates of Intrinsic Susceptibility-weighted MR Imaging before and during Chemotherapy, *Radiology*, 2010, **257**, 643, DOI: 10.1148/radiol.10100421.

82 J. Oh, R. G. Henry, A. Pirzkall, Y. Lu, X. Li, I. Catalaa, S. Chang, W. P. Dillon and S. J. Nelson, Survival analysis in patients with glioblastoma multiforme: predictive value of choline-to-*N*-acetylaspartate index, apparent diffusion coefficient, and relative cerebral blood volume, *J. Magn. Reson. Imaging*, 2004, **19**, 546–54, DOI: 10.1002/jmri.20039; R. G. Henry, D. B. Vigneron, N. J. Fischbein, P. E. Grant, M. R. Day, S. M. Noworolski, J. M. Star-Lack, L. L. Wald, W. P. Dillon, S. M. Chang and S. J. Nelson, Comparison of relative cerebral blood volume and proton spectroscopy in patients with treated gliomas, *AJNR Am. J. Neuroradiol.*, 2000, **21**, 357–66.

83 J. Kurhanewicz, M. G. Swanson, S. J. Nelson and D. B. Vigneron, Combined magnetic resonance imaging and spectroscopic imaging approach to molecular imaging of prostate cancer, *J. Magn. Reson. Imaging*, 2002, **16**, 451–63, DOI: 10.1002/jmri.10172; U. Sharma, A. Mehta, V. Seenu and N. R. Jagannathan, Biochemicalcharacterization of metastatic lymph nodes of breast cancer patients by *in vitro*^{1}H magnetic resonance spectroscopy: a pilot study, *Magn. Reson. Imaging*, 2004, **22**, 697–706, DOI: 10.1016/j.mri.2004.01.037.

84 G. M. Lanza, P. M. Winter, A. M. Neubauer, S. D. Caruthers, F. D. Hockett and S. A. Wickline, ^{1}H/^{19}F magnetic resonance molecular imaging with perfluorocarbon nanoparticles, *Curr. Top. Dev. Biol.*, 2005, **70**, 57–76, DOI: 10.1016/S0070-2153(05)70003-X.

85 C. A. Presant, W. Wolf, V. Waluch, C. Wiseman, P. Kennedy, D. Blayney and R. R. Brechner, Association of intratumoral pharmacokinetics of fluorouracil with clinical response, *Lancet*, 1994, **343**, 1184–7.

86 S. E. Day, M. I. Kettunen, F. A. Gallagher, D. E. Hu, M. Lerche, J. Wolber, K. Golman, J. H. Ardenkjaer-Larsen and K. M. Brindle, Detecting tumor response to treatment using hyperpolarized ^{13}C magnetic resonance imaging and spectroscopy, *Nat. Med.*, 2007, **13**, 1382–7, DOI: 10.1038/nm1650.

87 D. E. Jenkins, S. F. Yu, Y. S. Hornig, T. Purchio and P. R. Contag, *In vivo* monitoring of tumor relapse and metastasis

using bioluminescent PC-3M-luc-C6 cells in murine models of human prostate cancer, *Clin. Exp. Metastasis*, 2003, **20**, 745–56.
88 S. A. Boppart, B. E. Bouma, C. Pitris, G. J. Tearney, J. F. Southern, M. E. Brezinski and J. G. Fujimoto, Intraoperative assessment of microsurgery with three-dimensional optical coherence tomography, *Radiology*, 1998, **208**, 81–6.
89 E. S. Olson, T. Jiang, T. A. Aguilera, Q. T. Nguyen, L. G. Ellies, M. Scadeng and R. Y. Tsien, Activatable cell penetrating peptides linked to nanoparticles as dual probes for *in vivo* fluorescence and MR imaging of proteases, *Proc. Natl. Acad. Sci. U. S. A.*, 2010, **107**, 4311–6, DOI: 10.1073/pnas.0910283107.
90 F. Zhou, D. Xing, S. Wu and W. R. Chen, Intravital imaging of tumor apoptosis with FRET probes during tumor therapy, *Mol. Imaging Biol.*, 2009, **12**, 63–70, DOI: 10.1007/s11307-009-0235-y.
91 J. C. Jung and M. J. Schnitzer, Multiphoton endoscopy, *Opt. Lett.*, 2003, **28**, 902–4.
92 G. E. Weller, M. K. Wong, R. A. Modzelewski, E. Lu, A. L. Klibanov, W. R. Wagner and F. S. Villanueva, Ultrasonic imaging of tumor angiogenesis using contrast microbubbles targeted *via* the tumor-binding peptide arginine-arginine-leucine, *Cancer Res.*, 2005, **65**, 533–9.
93 T. J. Ruers, B. Wiering, J. R. van der Sijp, R. M. Roumen, K. P. de Jong, E. F. Comans, J. Pruim, H. M. Dekker, P. F. Krabbe and W. J. Oyen, Improved selection of patients for hepatic surgery of colorectal liver metastases with (18)F-FDG PET: a randomized study, *J. Nucl. Med.*, 2009, **50**, 1036–41, DOI: 10.2967/jnumed.109.063040.
94 D. A. Pierce and D. L. Preston, Risks from low doses of radiation, *Science*, 1996, **272**, 632–3.
95 M. Atri, New technologies and directed agents for applications of cancer imaging, *J. Clin. Oncol.*, 2006, **24**, 3299–308, DOI: 10.1200/JCO.2006.06.6159.
96 P. Therasse, S. G. Arbuck, E. A. Eisenhauer, J. Wanders, R. S. Kaplan, L. Rubinstein, J. Verweij, M. Van Glabbeke, A. T. van Oosterom, M. C. Christian and S. G. Gwyther, New guidelines to evaluate the response to treatment in solid tumors. European Organization for Research and Treatment of Cancer, National Cancer Institute of the United States, National Cancer Institute of Canada, *J. Natl. Cancer Inst.*, 2000, **92**, 205–16; P. Therasse, E. A. Eisenhauer and J. Verweij, RECIST revisited: a review of validation studies on tumour assessment, *Eur. J. Cancer*, 2006, **42**, 1031–9, DOI: 10.1016/j.ejca.2006.01.026.
97 T. Beyer, D. W. Townsend and T. M. Blodgett, Dual-modality PET/CT tomography for clinical oncology, *Q. J. Nucl. Med.*, 2002, **46**, 24–34.
98 D. Lardinois, W. Weder, T. F. Hany, E. M. Kamel, S. Korom, B. Seifert, G. K. von Schulthess and H. C. Steinert, Staging of non-small-cell lung cancer with integrated positron-emission tomography and computed tomography, *N. Engl. J. Med.*, 2003, **348**, 2500–7, DOI: 10.1056/NEJMoa022136; B. Fischer, U. Lassen, J. Mortensen, S. Larsen, A. Loft, A. Bertelsen, J. Ravn, P. Clementsen, A. Hogholm, K. Larsen, T. Rasmussen, S. Keiding, A. Dirksen, O. Gerke, B. Skov, I. Steffensen, H. Hansen, P. Vilmann, G. Jacobsen, V. Backer, N. Maltbaek, J. Pedersen, H. Madsen, H. Nielsen and L. Hojgaard, Preoperative staging of lung cancer with combined PET-CT, *N. Engl. J. Med.*, 2009, **361**, 32–9, DOI: 10.1056/NEJMoa0900043.
99 R. L. Wahl, H. Jacene, Y. Kasamon and M. A. Lodge, From RECIST to PERCIST: Evolving Considerations for PET response criteria in solid tumors, *J. Nucl. Med.*, 2009, **50**(Suppl 1), 122S–50S, DOI: 10.2967/jnumed.108.057307.
100 H. Young, R. Baum, U. Cremerius, K. Herholz, O. Hoekstra, A. A. Lammertsma, J. Pruim and P. Price, Measurement of clinical and subclinical tumour response using [^{18}F]-fluorodeoxy-glucose and positron emission tomography: review and 1999 EORTC recommendations. European Organization for Research and Treatment of Cancer (EORTC) PET Study Group, *Eur. J. Cancer*, 1999, **35**, 1773–82, DOI: 10.1016/S0959-8049(99)00229-4.
101 T. S. Koh, C. H. Thng, S. Hartono, P. S. Lee, S. P. Choo, D. Y. Poon, H. C. Toh and S. Bisdas, Dynamic contrast-enhanced CT imaging of hepatocellular carcinoma in cirrhosis: feasibility of a prolonged dual-phase imaging protocol with tracer kinetics modeling, *Eur. Radiol.*, 2009, **19**, 1184–96, DOI: 10.1007/s00330-008-1252-y; S. Bisdas, G. N. Konstantinou, P. S. Lee, C. H. Thng, J. Wagenblast, M. Baghi and T. S. Koh, Dynamic contrast-enhanced CT of head and neck tumors: perfusion measurements using a distributed-parameter tracer kinetic model. Initial results and comparison with deconvolution-based analysis, *Phys. Med. Biol.*, 2007, **52**, 6181–96, DOI: 10.1088/0031-9155/52/20/007.
102 M. L. Ah-See, A. Makris, N. J. Taylor, M. Harrison, P. I. Richman, R. J. Burcombe, J. J. Stirling, J. A. d'Arcy, D. J. Collins, M. R. Pittam, D. Ravichandran and A. R. Padhani, Early changes in functional dynamic magnetic resonance imaging predict for pathologic response to neo-adjuvant chemotherapy in primary breast cancer, *Clin. Cancer Res.*, 2008, **14**, 6580–9, DOI: 10.1158/1078-0432.CCR-07-4310; P. L. Choyke, A. J. Dwyer and M. V. Knopp, Functional tumor imaging with dynamic contrast-enhanced magnetic resonance imaging, *J. Magn. Reson. Imaging*, 2003, **17**, 509–20, DOI: 10.1002/jmri.10304.
103 H. W. van Laarhoven, W. Fiedler, I. M. Desar, J. J. van Asten, S. Marreaud, D. Lacombe, A. S. Govaerts, J. Bogaerts, P. Lasch, J. N. Timmer-Bonte, A. Lambiase, C. Bordignon, C. J. Punt, A. Heerschap and C. M. van Herpen, Phase I clinical and magnetic resonance imaging study of the vascular agent NGR-hTNF in patients with advanced cancers (European Organization for Research and Treatment of Cancer Study 16041), *Clin. Cancer Res.*, 2010, **16**, 1315–23, DOI: 10.1158/1078-0432.CCR-09-1621; J. Baar, P. Silverman, J. Lyons, P. Fu, F. Abdul-Karim, N. Ziats, J. Wasman, P. Hartman, J. Jesberger, L. Dumadag, E. Hohler, R. Leeming, R. Shenk, H. Chen, K. McCrae, A. Dowlati, S. C. Remick and B. Overmoyer, A vasculature-targeting regimen of preoperative docetaxel with or without bevacizumab for locally advanced breast cancer: impact on angiogenic biomarkers, *Clin. Cancer Res.*, 2009, **15**, 3583–90, DOI: 10.1158/1078-0432.CCR-08-2917; T. Meyer, A. M. Gaya, G. Dancey, M. R. Stratford, S. Othman, S. K. Sharma, D. Wellsted, N. J. Taylor, J. J. Stirling, L. Poupard, L. K. Folkes, P. S. Chan, R. B. Pedley, K. A. Chester, K. Owen, J. A. Violet, A. Malaroda, A. J. Green, J. Buscombe, A. R. Padhani, G. J. Rustin and R. H. Begent, A phase I trial of radioimmunotherapy with 131I-A5B7 anti-CEA antibody in combination with combretastatin-A4-phosphate in advanced gastrointestinal carcinomas, *Clin. Cancer Res.*, 2009, **15**, 4484–92, DOI: 10.1158/1078-0432.CCR-09-0035; O. M. Hahn, C. Yang, M. Medved, G. Karczmar, E. Kistner, T. Karrison, E. Manchen, M. Mitchell, M. J. Ratain and W. M. Stadler, Dynamic contrast-enhanced magnetic resonance imaging pharmacodynamic biomarker study of sorafenib in metastatic renal carcinoma, *J. Clin. Oncol.*, 2008, **26**, 4572–8, DOI: 10.1200/JCO.2007.15.5655; Q. S. Ng, V. Goh, J. Milner, M. R. Stratford, L. K. Folkes, G. M. Tozer, M. I. Saunders and P. J. Hoskin, Effect of nitric-oxide synthesis on tumour blood volume and vascular activity: a phase I study, *Lancet Oncol.*, 2007, **8**, 111–8, DOI: 10.1016/S1470-2045(07)70001-3; Q. S. Ng, V. Goh, D. Carnell, K. Meer, A. R. Padhani, M. I. Saunders and P. J. Hoskin, Tumor antivascular effects of radiotherapy combined with combretastatin a4 phosphate in human non-small-cell lung cancer, *Int. J. Radiat. Oncol., Biol., Phys.*, 2007, **67**, 1375–80, DOI: 10.1016/j.ijrobp.2006.11.028.
104 D. A. Hamstra, C. J. Galban, C. R. Meyer, T. D. Johnson, P. C. Sundgren, C. Tsien, T. S. Lawrence, L. Junck, D. J. Ross, A. Rehemtulla, B. D. Ross and T. L. Chenevert, Functional diffusion map as an early imaging biomarker for high-grade glioma: correlation with conventional radiologic response and overall survival, *J. Clin. Oncol.*, 2008, **26**, 3387–94, DOI: 10.1200/JCO.2007.15.2363; S. Kim, L. Loevner, H. Quon, E. Sherman, G. Weinstein, A. Kilger and H. Poptani, Diffusion-weighted magnetic resonance imaging for predicting and detecting early response to chemoradiation therapy of squamous cell carcinomas of the head and neck, *Clin. Cancer Res.*, 2009, **15**, 986–94, DOI: 10.1158/1078-0432.CCR-08-1287; Y. Cui, X. P. Zhang, Y. S. Sun, L. Tang and L. Shen, Apparent diffusion coefficient: potential imaging biomarker for prediction and early detection of response to chemotherapy in hepatic metastases, *Radiology*, 2008, **248**, 894–900, DOI: 10.1148/radiol.2483071407; W. Reichardt, E. Juettner, M. Uhl, D. V. Elverfeldt and U. Kontny, Diffusion-weighted imaging as predictor of therapy response in

an animal model of Ewing sarcoma, *Invest. Radiol.*, 2009, **44**, 298–303, DOI: 10.1097/RLI.0b013e31819dcc84.
105 A. R. Padhani and K. A. Miles, Multiparametric imaging of tumor response to therapy, *Radiology*, 2010, **256**, 348–64, DOI: 10.1148/radiol.10091760.
106 H. Ashamalla, S. Rafla, K. Parikh, B. Mokhtar, G. Goswami, S. Kambam, H. Abdel-Dayem, A. Guirguis, P. Ross and A. Evola, The contribution of integrated PET/CT to the evolving definition of treatment volumes in radiation treatment planning in lung cancer, *Int. J. Radiat. Oncol., Biol., Phys.*, 2005, **63**, 1016–23, DOI: 10.1016/j.ijrobp.2005.04.021.
107 E. Topkan, A. A. Yavuz, M. Aydin, C. Onal, F. Yapar and M. N. Yavuz, Comparison of CT and PET-CT based planning of radiation therapy in locally advanced pancreatic carcinoma, *J. Exp. Clin. Cancer Res.*, 2008, **27**, 41, DOI: 10.1186/1756-9966-27-41.
108 S. Tatli, V. H. Gerbaudo, M. Mamede, K. Tuncali, P. B. Shyn and S. G. Silverman, Abdominal masses sampled at PET/CT-guided percutaneous biopsy: initial experience with registration of prior PET/CT images, *Radiology*, 2010, **256**, 305–11, DOI: 10.1148/radiol.10090931.
109 E. J. Somer, P. K. Marsden, N. A. Benatar, J. Goodey, M. J. O'Doherty and M. A. Smith, PET-MR image fusion in soft tissue sarcoma: accuracy, reliability and practicality of interactive point-based and automated mutual information techniques, *Eur. J. Nucl. Med. Mol. Imaging*, 2003, **30**, 54–62.
110 E. S. Olson, T. Jiang, T. A. Aguilera, Q. T. Nguyen, L. G. Ellies, M. Scadeng and R. Y. Tsien, Activatable cell penetrating peptides linked to nanoparticles as dual probes for *in vivo* fluorescence and MR imaging of proteases, *Proc. Natl. Acad. Sci. U. S. A.*, 2010, **107**, 4311–6, DOI: 10.1073/pnas.0910283107.
111 M. Nahrendorf, E. Keliher, B. Marinelli, P. Waterman, P. F. Feruglio, L. Fexon, M. Pivovarov, F. K. Swirski, M. J. Pittet, C. Vinegoni and R. Weissleder, Hybrid PET-optical imaging using targeted probes, *Proc. Natl. Acad. Sci. U. S. A.*, 2010, **107**, 7910–5, DOI: 10.1073/pnas.0915163107.
112 M. Nahrendorf, H. Zhang, S. Hembrador, P. Panizzi, D. E. Sosnovik, E. Aikawa, P. Libby, F. K. Swirski and R. Weissleder, Nanoparticle PET-CT imaging of macrophages in inflammatory atherosclerosis, *Circulation*, 2008, **117**, 379–87, DOI: 10.1161/CIRCULATIONAHA.107.741181.
113 D. J. Slamon, G. M. Clark, S. G. Wong, W. J. Levin, A. Ullrich and W. L. McGuire, Human breast cancer: correlation of relapse and survival with amplification of the HER-2/neu oncogene, *Science*, 1987, **235**, 177–82.
114 E. E. Lower, E. Glass, R. Blau and S. Harman, HER-2/neu expression in primary and metastatic breast cancer, *Breast Cancer Res. Treat.*, 2009, **113**, 301–6, DOI: 10.1007/s10549-008-9931-6.
115 M. Brunelli, E. Manfrin, G. Martignoni, K. Miller, A. Remo, D. Reghellin, S. Bersani, S. Gobbo, A. Eccher, M. Chilosi and F. Bonetti, Genotypic intratumoral heterogeneity in breast carcinoma with HER2/neu amplification: evaluation according to ASCO/CAP criteria, *Am. J. Clin. Pathol.*, 2009, **131**, 678–82, DOI: 10.1309/AJCP09VUTZWZXBMJ.
116 Y. Tang, J. Wang, D. A. Scollard, H. Mondal, C. Holloway, H. J. Kahn and R. M. Reilly, Imaging of HER2/neu-positive BT-474 human breast cancer xenografts in athymic mice using (111)In-trastuzumab (Herceptin) Fab fragments, *Nucl. Med. Biol.*, 2005, **32**, 51–8, DOI: 10.1016/j.nucmedbio.2004.08.003.
117 T. A. Smith, Towards detecting the HER-2 receptor and metabolic changes induced by HER-2-targeted therapies using medical imaging, *Br. J. Radiol.*, 2010, **83**, 638–44, DOI: 10.1259/bjr/31053812.
118 A. Orlova, V. Tolmachev, R. Pehrson, M. Lindborg, T. Tran, M. Sandstrom, F. Y. Nilsson, A. Wennborg, L. Abrahmsen and J. Feldwisch, Synthetic affibody molecules: a novel class of affinity ligands for molecular imaging of HER2-expressing malignant tumors, *Cancer Res.*, 2007, **67**, 2178–86, DOI: 10.1158/0008-5472.CAN-06-2887.
119 R. P. Baum, V. Prasad, D. Muller, C. Schuchardt, A. Orlova, A. Wennborg, V. Tolmachev and J. Feldwisch, Molecular imaging of HER2-expressing malignant tumors in breast cancer patients using synthetic vIn- or ^{68}Ga-labeled affibody molecules, *J. Nucl. Med.*, 2010, **51**, 892–7, DOI: 10.2967/jnumed.109.073239.
120 A. C. Wolff, M. E. Hammond, J. N. Schwartz, K. L. Hagerty, D. C. Allred, R. J. Cote, M. Dowsett, P. L. Fitzgibbons, W. M. Hanna, A. Langer, L. M. McShane, S. Paik, M. D. Pegram, E. A. Perez, M. F. Press, A. Rhodes, C. Sturgeon, S. E. Taube, R. Tubbs, G. H. Vance, M. van de Vijver, T. M. Wheeler and D. F. Hayes, American Society of Clinical Oncology/College of American Pathologists guideline recommendations for human epidermal growth factor receptor 2 testing in breast cancer, *J. Clin. Oncol.*, 2007, **25**, 118–45, DOI: 10.1200/JCO.2006.09.2775.
121 P. Workman, Pharmacokinetics and cancer: successes, failures and future prospects, *Cancer Surv.*, 1993, **17**, 1–26; B. M. Seddon and P. Workman, The role of functional and molecular imaging in cancer drug discovery and development, *Br. J. Radiol.*, 2003, **76**(Spec. No. 2), S128–38.
122 D. M. Potter, Adaptive dose finding for phase I clinical trials of drugs used for chemotherapy of cancer, *Stat. Med.*, 2002, **21**, 1805–23, DOI: 10.1002/sim.1141.
123 M. J. Ratain, R. L. Schilsky, B. A. Conley and M. J. Egorin, Pharmacodynamics in cancer therapy, *J. Clin. Oncol.*, 1990, **8**, 1739–53.
124 A. J. Fischman, N. M. Alpert and R. H. Rubin, Pharmacokinetic imaging: a noninvasive method for determining drug distribution and action, *Clin. Pharmacokinet.*, 2002, **41**, 581–602, DOI: 10.2165/00003088-200241080-00003.
125 T. H. Chow, Y. Y. Lin, J. J. Hwang, H. E. Wang, Y. L. Tseng, V. F. Pang, R. S. Liu, W. J. Lin, C. S. Yang and G. Ting, Therapeutic efficacy evaluation of ^{111}In-labeled PEGylated liposomal vinorelbine in murine colon carcinoma with multi-modalities of molecular imaging, *J. Nucl. Med.*, 2009, **50**, 2073–81, DOI: 10.2967/jnumed.109.063503; W. Cai, K. Chen, L. He, Q. Cao, A. Koong and X. Chen, Quantitative PET of EGFR expression in xenograft-bearing mice using ^{64}Cu-labeled cetuximab, a chimeric anti-EGFR monoclonal antibody, *Eur. J. Nucl. Med. Mol. Imaging*, 2007, **34**, 850–8, DOI: 10.1007/s00259-006-0361-6.
126 G. Niu, Z. Li, Q. Cao and X. Chen, Monitoring therapeutic response of human ovarian cancer to 17-DMAG by noninvasive PET imaging with (64)Cu-DOTA-trastuzumab, *Eur. J. Nucl. Med. Mol. Imaging*, 2009, **36**, 1510–9, DOI: 10.1007/s00259-009-1158-1.
127 I. R. Wilding and J. A. Bell, Improved early clinical development through human microdosing studies, *Drug Discovery Today*, 2005, **10**, 890–4, DOI: 10.1016/S1359-6446(05)03509-9.
128 T. H. Oude Munnink, M. A. Korte, W. B. Nagengast, H. Timmer-Bosscha, C. P. Schroder, J. R. Jong, G. A. Dongen, M. R. Jensen, C. Quadt, M. N. Hooge and E. G. Vries, (89)Zr-trastuzumab PET visualises HER2 downregulation by the HSP90 inhibitor NVP-AUY922 in a human tumour xenograft, *Eur. J. Cancer*, 2010, **46**, 678–84, DOI: 10.1016/j.ejca.2009.12.009.
129 A. Citri, I. Alroy, S. Lavi, C. Rubin, W. Xu, N. Grammatikakis, C. Patterson, L. Neckers, D. W. Fry and Y. Yarden, Drug-induced ubiquitylation and degradation of ErbB receptor tyrosine kinases: implications for cancer therapy, *EMBO J.*, 2002, **21**, 2407–17, DOI: 10.1093/emboj/21.10.2407.
130 E. C. Dijkers, T. H. Oude Munnink, J. G. Kosterink, A. H. Brouwers, P. L. Jager, J. R. de Jong, G. A. van Dongen, C. P. Schroder, M. N. Lub-de Hooge and E. G. de Vries, Biodistribution of ^{89}Zr-trastuzumab and PET imaging of HER2-positive lesions in patients with metastatic breast cancer, *Clin. Pharmacol. Ther.*, 2010, **87**, 586–92, DOI: 10.1038/clpt.2010.12.
131 R. Katz, Biomarkers and surrogate markers: an FDA perspective, *NeuroRx*, 2004, **1**, 189–95.
132 M. M. Gottesman, How cancer cells evade chemotherapy: sixteenth Richard and Hinda Rosenthal Foundation Award Lecture, *Cancer Res.*, 1993, **53**, 747–54; S. W. Lowe, H. E. Ruley, T. Jacks and D. E. Housman, p53-dependent apoptosis modulates the cytotoxicity of anticancer agents, *Cell*, 1993, **74**, 957–67, DOI: 10.1016/0092-8674(93)90719-7.
133 S. Kraljevic, M. Sedic, M. Scott, P. Gehrig, R. Schlapbach and K. Pavelic, Casting light on molecular events underlying anti-cancer drug treatment: what can be seen from the proteomics

point of view?, *Cancer Treat. Rev.*, 2006, **32**, 619–29, DOI: 10.1016/j.ctrv.2006.09.002.
134 A. Trumpp and O. D. Wiestler, Mechanisms of Disease: cancer stem cells[mdash]targeting the evil twin, *Nat. Clin. Pract. Oncol.*, 2008, **5**, 337–347; R. M. Glasspool, J. M. Teodoridis and R. Brown, Epigenetics as a mechanism driving polygenic clinical drug resistance, *Br. J. Cancer*, 2006, **94**, 1087–1092.
135 L. A. Carey, E. C. Dees, L. Sawyer, L. Gatti, D. T. Moore, F. Collichio, D. W. Ollila, C. I. Sartor, M. L. Graham and C. M. Perou, The triple negative paradox: primary tumor chemosensitivity of breast cancer subtypes, *Clin. Cancer Res.*, 2007, **13**, 2329–34, DOI: 10.1158/1078-0432.CCR-06-1109; V. C. Hodgkinson, G. L. Eagle, P. J. Drew, M. J. Lind and L. Cawkwell, Biomarkers of chemotherapy resistance in breast cancer identified by proteomics: current status, *Cancer Lett.*, 2010, **294**, 13–24, DOI: 10.1016/j.canlet.2010.01.036.
136 P. Kannan, C. John, S. S. Zoghbi, C. Halldin, M. M. Gottesman, R. B. Innis and M. D. Hall, Imaging the function of P-glycoprotein with radiotracers: pharmacokinetics and *in vivo* applications, *Clin. Pharmacol. Ther.*, 2009, **86**, 368–77, DOI: 10.1038/clpt.2009.138.
137 M. Fellner, W. Dillenburg, H. G. Buchholz, N. Bausbacher, M. Schreckenberger, F. Renz, F. Rosch and O. Thews, Assessing p-Glycoprotein (Pgp) Activity *in vivo* Utilizing (68)Ga-Schiff Base Complexes, *Mol. Imaging Biol.*, 2010, DOI: 10.1007/s11307-010-0410-1; C. M. Gomes, A. J. Abrunhosa, E. K. Pauwels and M. F. Botelho, P-glycoprotein *versus* MRP1 on transport kinetics of cationic lipophilic substrates: a comparative study using [^{99m}Tc]sestamibi and [^{99m}Tc]tetrofosmin, *Cancer Biother. Radiopharm.*, 2009, **24**, 215–27, DOI: 10.1089/cbr.2008.0539; N. H. Hendrikse and W. Vaalburg, Imaging of P glycoprotein function *in vivo* with PET, *Novartis Found. Symp.*, 2002, **243**, 137–45, DOI: 10.1002/0470846356.ch10; discussion 145-8, 180-5.
138 S. V. Sharma, D. Y. Lee, B. Li, M. P. Quinlan, F. Takahashi, S. Maheswaran, U. McDermott, N. Azizian, L. Zou, M. A. Fischbach, K.-K. Wong, K. Brandstetter, B. Wittner, S. Ramaswamy, M. Classon and J. Settleman, A Chromatin-Mediated Reversible Drug-Tolerant State in Cancer Cell Subpopulations, *Cell*, 2010, **141**, 69–80.
139 D. Cunningham, Y. Humblet, S. Siena, D. Khayat, H. Bleiberg, A. Santoro, D. Bets, M. Mueser, A. Harstrick, C. Verslype, I. Chau and E. Van Cutsem, Cetuximab monotherapy and cetuximab plus irinotecan in irinotecan-refractory metastatic colorectal cancer, *N. Engl. J. Med.*, 2004, **351**, 337–45, DOI: 10.1056/NEJMoa033025.
140 J. Souglakos, A. Kalykaki, L. Vamvakas, N. Androulakis, K. Kalbakis, S. Agelaki, N. Vardakis, M. Tzardi, A. P. Kotsakis, J. Gioulbasanis, D. Tsetis, G. Sfakiotaki, D. Chatzidaki, D. Mavroudis and V. Georgoulias, Phase II trial of capecitabine and oxaliplatin (CAPOX) plus cetuximab in patients with metastatic colorectal cancer who progressed after oxaliplatin-based chemotherapy, *Ann. Oncol.*, 2007, **18**, 305–10, DOI: 10.1093/annonc/mdl392.
141 E. Pasquier, M. Kavallaris and N. Andre, Metronomic chemotherapy: new rationale for new directions, *Nat. Rev. Clin. Oncol.*, 2010, **7**, 455–65, DOI: 10.1038/nrclinonc.2010.82; R. S. Kerbel and B. A. Kamen, The anti-angiogenic basis of metronomic chemotherapy, *Nat. Rev. Cancer*, 2004, **4**, 423–36, DOI: 10.1038/nrc1369.
142 G. Gasparini, Metronomic scheduling: the future of chemotherapy?, *Lancet Oncol.*, 2001, **2**, 733–40, DOI: 10.1016/S1470-2045(01)00587-3.
143 R. Lord, S. Nair, A. Schache, J. Spicer, N. Somaihah, V. Khoo and H. Pandha, Low dose metronomic oral cyclophosphamide for hormone resistant prostate cancer: a phase II study, *J. Urol.*, 2007, **177**, 2136–40, DOI: 10.1016/j.juro.2007.01.143; discussion 2140.
144 J. M. Jurado, A. Sanchez, B. Pajares, E. Perez, L. Alonso and E. Alba, Combined oral cyclophosphamide and bevacizumab in heavily pre-treated ovarian cancer, *Clin. Transl. Oncol.*, 2008, **10**, 583–6, DOI: 10.1007/s12094-008-0254-7.
145 M. Colleoni, A. Rocca, M. T. Sandri, L. Zorzino, G. Masci, F. Nole, G. Peruzzotti, C. Robertson, L. Orlando, S. Cinieri, B. F. de, G. Viale and A. Goldhirsch, Low-dose oral methotrexate and cyclophosphamide in metastatic breast cancer: antitumor activity and correlation with vascular endothelial growth factor levels, *Ann. Oncol.*, 2002, **13**, 73–80; S. Dellapasqua, F. Bertolini, V. Bagnardi, E. Campagnoli, E. Scarano, R. Torrisi, Y. Shaked, P. Mancuso, A. Goldhirsch, A. Rocca, E. Pietri and M. Colleoni, Metronomic cyclophosphamide and capecitabine combined with bevacizumab in advanced breast cancer, *J. Clin. Oncol.*, 2008, **26**, 4899–905, DOI: 10.1200/JCO.2008.17.4789.
146 S. F. Rosebrough, Two-step immunological approaches for imaging and therapy, *Q. J. Nucl. Med.*, 1996, **40**, 234–51.
147 C. Bremer, S. Bredow, U. Mahmood, R. Weissleder and C. H. Tung, Optical imaging of matrix metalloproteinase-2 activity in tumors: feasibility study in a mouse model, *Radiology*, 2001, **221**, 523–9.
148 G. Lucignani and M. Rodriguez-Porcel, *In vivo* imaging for stem cell therapy: new developments and future challenges, *Eur. J. Nucl. Med. Mol. Imaging*, 2011, **38**, 400–5, DOI: 10.1007/s00259-010-1695-7; M. Rodriguez-Porcel, *In vivo* imaging and monitoring of transplanted stem cells: clinical applications, *Curr. Cardiol. Rep.*, 2010, **12**, 51–8, DOI: 10.1007/s11886-009-0073-1; R. Schafer, R. Bantleon, R. Kehlbach, G. Siegel, J. Wiskirchen, H. Wolburg, T. Kluba, F. Eibofner, H. Northoff, C. D. Claussen and H. P. Schlemmer, Functional investigations on human mesenchymal stem cells exposed to magnetic fields and labeled with clinically approved iron nanoparticles, *BMC Cell Biol.*, 2010, **11**, 22, DOI: 10.1186/1471-2121-11-22; T. Higuchi, M. Anton, A. Saraste, K. Dumler, J. Pelisek, S. G. Nekolla, F. M. Bengel and M. Schwaiger, Reporter gene PET for monitoring survival of transplanted endothelial progenitor cells in the rat heart after pretreatment with VEGF and atorvastatin, *J. Nucl. Med.*, 2009, **50**, 1881–6, DOI: 10.2967/jnumed.109.067801.
149 M. A. Rueger, H. Backes, M. Walberer, B. Neumaier, R. Ullrich, M. L. Simard, B. Emig, G. R. Fink, M. Hoehn, R. Graf and M. Schroeter, Noninvasive imaging of endogenous neural stem cell mobilization *in vivo* using positron emission tomography, *J. Neurosci.*, 2010, **30**, 6454–60, DOI: 10.1523/JNEUROSCI.6092-09.2010.
150 J. K. Willmann, R. Paulmurugan, M. Rodriguez-Porcel, W. Stein, T. J. Brinton, A. J. Connolly, C. H. Nielsen, A. M. Lutz, J. Lyons, F. Ikeno, Y. Suzuki, J. Rosenberg, I. Y. Chen, J. C. Wu, A. C. Yeung, P. Yock, R. C. Robbins and S. S. Gambhir, Imaging gene expression in human mesenchymal stem cells: from small to large animals, *Radiology*, 2009, **252**, 117–27, DOI: 10.1148/radiol.2513081616.
151 I. Penuelas, G. Mazzolini, J. F. Boan, B. Sangro, J. Marti-Climent, M. Ruiz, J. Ruiz, N. Satyamurthy, C. Qian, J. R. Barrio, M. E. Phelps, J. A. Richter, S. S. Gambhir and J. Prieto, Positron emission tomography imaging of adenoviral-mediated transgene expression in liver cancer patients, *Gastroenterology*, 2005, **128**, 1787–95, DOI: 10.1053/j.gastro.2005.03.024.
152 S. S. Yaghoubi, M. C. Jensen, N. Satyamurthy, S. Budhiraja, D. Paik, J. Czernin and S. S. Gambhir, Noninvasive detection of therapeutic cytolytic T cells with ^{18}F-FHBG PET in a patient with glioma, *Nat. Clin. Pract. Oncol.*, 2009, **6**, 53–8, DOI: 10.1038/ncponc1278.
153 C. Tsurumi, N. Esser, E. Firat, S. Gaedicke, M. Follo, M. Behe, U. Elsasser-Beile, A. L. Grosu, R. Graeser and G. Niedermann, Non-invasive *in vivo* imaging of tumor-associated CD133/prominin, *PLoS One*, 2010, **5**, e15605, DOI: 10.1371/journal.pone.0015605.
154 A. Weigmann, D. Corbeil, A. Hellwig and W. B. Huttner, Prominin, a novel microvilli-specific polytopic membrane protein of the apical surface of epithelial cells, is targeted to plasmalemmal protrusions of non-epithelial cells, *Proc. Natl. Acad. Sci. U. S. A.*, 1997, **94**, 12425–30; K. Kemper, M. R. Sprick, M. de Bree, A. Scopelliti, L. Vermeulen, M. Hoek, J. Zeilstra, S. T. Pals, H. Mehmet, G. Stassi and J. P. Medema, The AC133 epitope, but not the CD133 protein, is lost upon cancer stem cell differentiation, *Cancer Res.*, 2010, **70**, 719–29, DOI: 10.1158/0008-5472.CAN-09-1820; S. K. Singh, I. D. Clarke, M. Terasaki, V. E. Bonn, C. Hawkins, J. Squire and P. B. Dirks, Identification of a cancer stem cell in human brain tumors, *Cancer Res.*, 2003, **63**, 5821–8; G. Ferrandina, M. Petrillo, G. Bonanno and G. Scambia, Targeting CD133 antigen in cancer, *Expert Opin. Ther. Targets*, 2009, **13**, 823–37, DOI: 10.1517/14728220903005616.

155 A. Pal, A. Glekas, M. Doubrovin, J. Balatoni, M. Namavari, T. Beresten, D. Maxwell, S. Soghomonyan, A. Shavrin, L. Ageyeva, R. Finn, S. M. Larson, W. Bornmann and J. G. Gelovani, Molecular imaging of EGFR kinase activity in tumors with 124I-labeled small molecular tracer and positron emission tomography, *Mol. Imaging Biol.*, 2006, **8**, 262–77, DOI: 10.1007/s11307-006-0049-0.
156 J. M. Perez, L. Josephson and R. Weissleder, Use of magnetic nanoparticles as nanosensors to probe for molecular interactions, *ChemBioChem*, 2004, **5**, 261–4, DOI: 10.1002/cbic.200300730.
157 H. K. Sajja, M. P. East, H. Mao, Y. A. Wang, S. Nie and L. Yang, Development of multifunctional nanoparticles for targeted drug delivery and noninvasive imaging of therapeutic effect, *Curr. Drug Discovery Technol.*, 2009, **6**, 43–51.
158 C. G. Hadjipanayis, R. Machaidze, M. Kaluzova, L. Wang, A. J. Schuette, H. Chen, X. Wu and H. Mao, EGFRvIII antibody-conjugated iron oxide nanoparticles for magnetic resonance imaging-guided convection-enhanced delivery and targeted therapy of glioblastoma, *Cancer Res.*, 2010, **70**, 6303–12, DOI: 10.1158/0008-5472.CAN-10-1022.
159 E. A. O'Flynn, A. R. Wilson and M. J. Michell, Image-guided breast biopsy: state-of-the-art, *Clin. Radiol.*, 2010, **65**, 259–70, DOI: 10.1016/j.crad.2010.01.008.
160 C. E. Mountford, R. L. Somorjai, P. Malycha, L. Gluch, C. Lean, P. Russell, B. Barraclough, D. Gillett, U. Himmelreich, B. Dolenko, A. E. Nikulin and I. C. Smith, Diagnosis and prognosis of breast cancer by magnetic resonance spectroscopy of fine-needle aspirates analysed using a statistical classification strategy, *Br. J. Surg.*, 2001, **88**, 1234–40, DOI: 10.1046/j.0007-1323.2001.01864.x.
161 C. Mountford, S. Ramadan, P. Stanwell and P. Malycha, Proton MRS of the breast in the clinical setting, *NMR Biomed.*, 2009, **22**, 54–64, DOI: 10.1002/nbm.1301.
162 B. Turkbey, P. A. Pinto and P. L. Choyke, Imaging techniques for prostate cancer: implications for focal therapy, *Nat. Rev. Urol.*, 2009, **6**, 191–203, DOI: 10.1038/nrurol.2009.27.
163 D. L. Langer, T. H. van der Kwast, A. J. Evans, J. Trachtenberg, B. C. Wilson and M. A. Haider, Prostate cancer detection with multi-parametric MRI: logistic regression analysis of quantitative T2, diffusion-weighted imaging, and dynamic contrast-enhanced MRI, *J. Magn. Reson. Imaging*, 2009, **30**, 327–34, DOI: 10.1002/jmri.21824.
164 R. C. Susil, C. Menard, A. Krieger, J. A. Coleman, K. Camphausen, P. Choyke, G. Fichtinger, L. L. Whitcomb, C. N. Coleman and E. Atalar, Transrectal prostate biopsy and fiducial marker placement in a standard 1.5 T magnetic resonance imaging scanner, *J. Urol.*, 2006, **175**, 113–20, DOI: 10.1016/S0022-5347(05)00065-0; A. V. D'Amico, C. M. Tempany, R. Cormack, N. Hata, M. Jinzaki, K. Tuncali, M. Weinstein and J. P. Richie, Transperineal magnetic resonance image guided prostate biopsy, *J. Urol.*, 2000, **164**, 385–7, DOI: 10.1016/S0022-5347(05)67366-1.
165 A. K. Singh, J. Kruecker, S. Xu, N. Glossop, P. Guion, K. Ullman, P. L. Choyke and B. J. Wood, Initial clinical experience with real-time transrectal ultrasonography-magnetic resonance imaging fusion-guided prostate biopsy, *BJU Int.*, 2008, **101**, 841–5, DOI: 10.1111/j.1464-410X.2007.07348.x; B. Turkbey, S. Xu, J. Kruecker, J. Locklin, Y. Pang, M. Bernardo, M. J. Merino, B. J. Wood, P. L. Choyke and P. A. Pinto, Documenting the location of prostate biopsies with image fusion, *BJU Int.*, 2011, **107**, 53, DOI: 10.1111/j.1464-410X.2010.09483.x.
166 S. Xu, J. Kruecker, B. Turkbey, N. Glossop, A. K. Singh, P. Choyke, P. Pinto and B. J. Wood, Real-time MRI-TRUS fusion for guidance of targeted prostate biopsies, *Comput.-Aided Surg.*, 2008, **13**, 255–64, DOI: 10.3109/10929080802364645.
167 B. Klaeser, J. Wiskirchen, J. Wartenberg, T. Weitzel, R. A. Schmid, M. D. Mueller and T. Krause, PET/CT-guided biopsies of metabolically active bone lesions: applications and clinical impact, *Eur. J. Nucl. Med. Mol. Imaging*, 2010, **37**, 2027, DOI: 10.1007/s00259-010-1524-z.
168 P. R. B. Mark I. Rowley, Anthony Coolen and Borivoj Vojnovic, in *BIOS, SPIE Photonics West*, The Moscone Center, San Francisco, California, USA, 2011, pp. 7903–74.
169 M. Offterdinger and P. I. Bastiaens, Prolonged EGFR signaling by ERBB2-mediated sequestration at the plasma membrane, *Traffic*, 2008, **9**, 147–55.
170 R. E. Itoh, K. Kurokawa, A. Fujioka, A. Sharma, B. J. Mayer and M. Matsuda, A FRET-based probe for epidermal growth factor receptor bound non-covalently to a pair of synthetic amphipathic helixes, *Exp. Cell Res.*, 2005, **307**, 142–52, DOI: 10.1016/j.yexcr.2005.02.026.
171 A. Y. Ting, K. H. Kain, R. L. Klemke and R. Y. Tsien, Genetically encoded fluorescent reporters of protein tyrosine kinase activities in living cells, *Proc. Natl. Acad. Sci. U. S. A.*, 2001, **98**, 15003–8, DOI: 10.1073/pnas.211564598; J. Zhang, R. E. Campbell, A. Y. Ting and R. Y. Tsien, Creating new fluorescent probes for cell biology, *Nat. Rev. Mol. Cell Biol.*, 2002, **3**, 906–18, DOI: 10.1038/nrm976; R. B. Sekar and A. Periasamy, Fluorescence resonance energy transfer (FRET) microscopy imaging of live cell protein localizations, *J. Cell Biol.*, 2003, **160**, 629–33, DOI: 10.1083/jcb.200210140; M. Peter, S. M. Ameer-Beg, M. K. Hughes, M. D. Keppler, S. Prag, M. Marsh, B. Vojnovic and T. Ng, Multiphoton-FLIM quantification of the EGFP-mRFP1 FRET pair for localization of membrane receptor-kinase interactions, *Biophys. J.*, 2005, **88**, 1224–37, DOI: 10.1529/biophysj.104.050153; J. R. Morris, C. Boutell, M. Keppler, R. Densham, D. Weekes, A. Alamshah, L. Butler, Y. Galanty, L. Pangon, T. Kiuchi, T. Ng and E. Solomon, The SUMO modification pathway is involved in the BRCA1 response to genotoxic stress, *Nature*, 2009, **462**, 886–90, DOI: 10.1038/nature08593; A. Kong, V. Calleja, P. Leboucher, A. Harris, P. J. Parker and B. Larijani, HER2 oncogenic function escapes EGFR tyrosine kinase inhibitors *via* activation of alternative HER receptors in breast cancer cells, *PLoS One*, 2008, **3**, e2881, DOI: 10.1371/journal.pone.0002881; G. Fruhwirth, D. R. Matthews, A. Brock, M. Keppler, B. Vojnovic, T. Ng, S. M. Ameer-Beg, presented in part at SPIE BIOS/Photonics West 2009, Yea.
172 M. Peter and S. M. Ameer-Beg, Imaging molecular interactions by multiphoton FLIM, *Biol. Cell*, 2004, **96**, 231–6, DOI: 10.1016/j.biolcel.2003.12.006; T. Forster, in *Modern Quantum Chemistry*, ed. Sinanoglu, Academic Press, New York, 1965, vol. III, pp. 93–137.
173 G. O. Fruhwirth, S. Ameer-Beg, R. Cook, T. Watson, T. Ng and F. Festy, Fluorescence lifetime endoscopy using TCSPC for the measurement of FRET in live cells, *Opt. Express*, 2010, **18**, 11148–58, DOI: 10.1364/OE.18.011148.
174 S. Urbe, J. McCullough, P. Row, I. A. Prior, R. Welchman and M. J. Clague, Control of growth factor receptor dynamics by reversible ubiquitination, *Biochem. Soc. Trans.*, 2006, **34**, 754–6, DOI: 10.1042/BST0340754.
175 M. J. Clague and S. Urbe, Multivesicular bodies, *Curr. Biol.*, 2008, **18**, R402–4, DOI: 10.1016/j.cub.2008.02.068.
176 B. Schoeberl, E. A. Pace, J. B. Fitzgerald, B. D. Harms, L. Xu, L. Nie, B. Linggi, A. Kalra, V. Paragas, R. Bukhalid, V. Grantcharova, N. Kohli, K. A. West, M. Leszczyniecka, M. J. Feldhaus, A. J. Kudla and U. B. Nielsen, Therapeutically targeting ErbB3: a key node in ligand-induced activation of the ErbB receptor-PI3K axis, *Sci. Signaling*, 2009, **2**, ra31, DOI: 10.1126/scisignal.2000352.
177 A. Guo, J. Villen, J. Kornhauser, K. A. Lee, M. P. Stokes, K. Rikova, A. Possemato, J. Nardone, G. Innocenti, R. Wetzel, Y. Wang, J. MacNeill, J. Mitchell, S. P. Gygi, J. Rush, R. D. Polakiewicz and M. J. Comb, Signaling networks assembled by oncogenic EGFR and c-Met, *Proc. Natl. Acad. Sci. U. S. A.*, 2008, **105**, 692–7, DOI: 10.1073/pnas.0707270105.
178 J. A. Engelman, K. Zejnullahu, T. Mitsudomi, Y. Song, C. Hyland, J. O. Park, N. Lindeman, C. M. Gale, X. Zhao, J. Christensen, T. Kosaka, A. J. Holmes, A. M. Rogers, F. Cappuzzo, T. Mok, C. Lee, B. E. Johnson, L. C. Cantley and P. A. Janne, MET amplification leads to gefitinib resistance in lung cancer by activating ERBB3 signaling, *Science*, 2007, **316**, 1039–43, DOI: 10.1126/science.1141478.
179 M. P. Gordon, T. Ha and P. R. Selvin, Single-molecule high-resolution imaging with photobleaching, *Proc. Natl. Acad. Sci. U. S. A.*, 2004, **101**, 6462–5, DOI: 10.1073/pnas.0401638101.
180 E. Toprak and P. R. Selvin, New fluorescent tools for watching nanometer-scale conformational changes of single molecules,

Annu. Rev. Biophys. Biomol. Struct., 2007, **36**, 349–69, DOI: 10.1146/annurev.biophys.36.040306.132700; L. S. Churchman, Z. Okten, R. S. Rock, J. F. Dawson and J. A. Spudich, Single molecule high-resolution colocalization of Cy3 and Cy5 attached to macromolecules measures intramolecular distances through time, *Proc. Natl. Acad. Sci. U. S. A.*, 2005, **102**, 1419–23, DOI: 10.1073/pnas.0409487102.

181 Y. Mosesson, G. B. Mills and Y. Yarden, Derailed endocytosis: an emerging feature of cancer, *Nat. Rev. Cancer*, 2008, **8**, 835–50; K. Shtiegman, B. S. Kochupurakkal, Y. Zwang, G. Pines, A. Starr, A. Vexler, A. Citri, M. Katz, S. Lavi, Y. Ben-Basat, S. Benjamin, S. Corso, J. Gan, R. B. Yosef, S. Giordano and Y. Yarden, Defective ubiquitinylation of EGFR mutants of lung cancer confers prolonged signaling, *Oncogene*, 2007, **26**, 6968–6978.

182 O. Zach and D. Lutz, Tumor cell detection in peripheral blood and bone marrow, *Curr. Opin. Oncol.*, 2006, **18**, 48–56, DOI: 10.1097/01.cco.0000198973.51615.fa.

183 K. Pantel, R. H. Brakenhoff and B. Brandt, Detection, clinical relevance and specific biological properties of disseminating tumour cells, *Nat. Rev. Cancer*, 2008, **8**, 329–40, DOI: 10.1038/nrc2375.

184 S. Braun, F. D. Vogl, B. Naume, W. Janni, M. P. Osborne, R. C. Coombes, G. Schlimok, I. J. Diel, B. Gerber, G. Gebauer, J. Y. Pierga, C. Marth, D. Oruzio, G. Wiedswang, E. F. Solomayer, G. Kundt, B. Strobl, T. Fehm, G. Y. Wong, J. Bliss, A. Vincent-Salomon and K. Pantel, A pooled analysis of bone marrow micrometastasis in breast cancer, *N. Engl. J. Med.*, 2005, **353**, 793–802, DOI: 10.1056/NEJMoa050434.

185 S. Nagrath, L. V. Sequist, S. Maheswaran, D. W. Bell, D. Irimia, L. Ulkus, M. R. Smith, E. L. Kwak, S. Digumarthy, A. Muzikansky, P. Ryan, U. J. Balis, R. G. Tompkins, D. A. Haber and M. Toner, Isolation of rare circulating tumour cells in cancer patients by microchip technology, *Nature*, 2007, **450**, 1235–9, DOI: 10.1038/nature06385.

186 G. T. Budd, M. Cristofanilli, M. J. Ellis, A. Stopeck, E. Borden, M. C. Miller, J. Matera, M. Repollet, G. V. Doyle, L. W. Terstappen and D. F. Hayes, Circulating tumor cells *versus* imaging–predicting overall survival in metastatic breast cancer, *Clin. Cancer Res.*, 2006, **12**, 6403–9, DOI: 10.1158/1078-0432.CCR-05-1769.

187 M. Balic, H. Lin, L. Young, D. Hawes, A. Giuliano, G. McNamara, R. H. Datar and R. J. Cote, Most early disseminated cancer cells detected in bone marrow of breast cancer patients have a putative breast cancer stem cell phenotype, *Clin. Cancer Res.*, 2006, **12**, 5615–21, DOI: 10.1158/1078-0432.CCR-06-0169.

188 K. Pantel, C. Alix-Panabieres and S. Riethdorf, Cancer micrometastases, *Nat. Rev. Clin. Oncol.*, 2009, **6**, 339–51, DOI: 10.1038/nrclinonc.2009.44.

189 J. Galon, A. Costes, F. Sanchez-Cabo, A. Kirilovsky, B. Mlecnik, C. Lagorce-Pages, M. Tosolini, M. Camus, A. Berger, P. Wind, F. Zinzindohoue, P. Bruneval, P. H. Cugnenc, Z. Trajanoski, W. H. Fridman and F. Pages, Type, density, and location of immune cells within human colorectal tumors predict clinical outcome, *Science*, 2006, **313**, 1960–4, DOI: 10.1126/science.1129139.

190 A. Hemsen, L. Riethdorf, N. Brunner, J. Berger, S. Ebel, C. Thomssen, F. Janicke and K. Pantel, Comparative evaluation of urokinase-type plasminogen activator receptor expression in primary breast carcinomas and on metastatic tumor cells, *Int. J. Cancer*, 2003, **107**, 903–9, DOI: 10.1002/ijc.11488; N. Reimers, K. Zafrakas, V. Assmann, C. Egen, L. Riethdorf, S. Riethdorf, J. Berger, S. Ebel, F. Janicke, G. Sauter and K. Pantel, Expression of extracellular matrix metalloproteases inducer on micrometastatic and primary mammary carcinoma cells, *Clin. Cancer Res.*, 2004, **10**, 3422–8, DOI: 10.1158/1078-0432.CCR-03-0610.

191 N. L. Komarova and D. Wodarz, Drug resistance in cancer: principles of emergence and prevention, *Proc. Natl. Acad. Sci. U. S. A.*, 2005, **102**, 9714–9, DOI: 10.1073/pnas.0501870102.

192 C. L. Sawyers, Calculated resistance in cancer, *Nat. Med.*, 2005, **11**, 824–5, DOI: 10.1038/nm0805-824.

193 A. M. Xu and P. H. Huang, Receptor tyrosine kinase coactivation networks in cancer, *Cancer Res.*, 2010, **70**, 3857–60, DOI: 10.1158/0008-5472.CAN-10-0163.

194 X. Huang, L. Gao, S. Wang, J. L. McManaman, A. D. Thor, X. Yang, F. J. Esteva and B. Liu, Heterotrimerization of the growth factor receptors erbB2, erbB3, and insulin-like growth factor-i receptor in breast cancer cells resistant to herceptin, *Cancer Res.*, 2010, **70**, 1204–14, DOI: 10.1158/0008-5472.CAN-09-3321.

195 J. M. Stommel, A. C. Kimmelman, H. Ying, R. Nabioullin, A. H. Ponugoti, R. Wiedemeyer, A. H. Stegh, J. E. Bradner, K. L. Ligon, C. Brennan, L. Chin and R. A. DePinho, Coactivation of receptor tyrosine kinases affects the response of tumor cells to targeted therapies, *Science*, 2007, **318**, 287–90, DOI: 10.1126/science.1142946.

196 G. Fruhwirth, L. Fernandez, G. Weitsman, G. S. Patel, M. T. Kelleher, A. Brock, S. Poland, D. R. Matthews, G. Keri, P. R. Barber, B. Vojnovic, S. M. Ameer-Beg, K. Lawler, A. Coolen, F. Fraternali and T. Ng, The use of Förster resonance energy transfer (FRET) to understand human proteome function: from studying networks to intravital imaging of cancer metastasis. ChemPhysChem, *ChemPhysChem*, 2011, **12**, 442–461, DOI: 10.1002/cphc.201000866.

197 T. Sorlie, R. Tibshirani, J. Parker, T. Hastie, J. S. Marron, A. Nobel, S. Deng, H. Johnsen, R. Pesich, S. Geisler, J. Demeter, C. M. Perou, P. E. Lonning, P. O. Brown, A. L. Borresen-Dale and D. Botstein, Repeated observation of breast tumor subtypes in independent gene expression data sets, *Proc. Natl. Acad. Sci. U. S. A.*, 2003, **100**, 8418–23, DOI: 10.1073/pnas.0932692100; J. S. Parker, M. Mullins, M. C. Cheang, S. Leung, D. Voduc, T. Vickery, S. Davies, C. Fauron, X. He, Z. Hu, J. F. Quackenbush, I. J. Stijleman, J. Palazzo, J. S. Marron, A. B. Nobel, E. Mardis, T. O. Nielsen, M. J. Ellis, C. M. Perou and P. S. Bernard, Supervised risk predictor of breast cancer based on intrinsic subtypes, *J. Clin. Oncol.*, 2009, **27**, 1160–7, DOI: 10.1200/JCO.2008.18.1370; Z. Hu, C. Fan, D. S. Oh, J. S. Marron, X. He, B. F. Qaqish, C. Livasy, L. A. Carey, E. Reynolds, L. Dressler, A. Nobel, J. Parker, M. G. Ewend, L. R. Sawyer, J. Wu, Y. Liu, R. Nanda, M. Tretiakova, A. Ruiz Orrico, D. Dreher, J. P. Palazzo, L. Perreard, E. Nelson, M. Mone, H. Hansen, M. Mullins, J. F. Quackenbush, M. J. Ellis, O. I. Olopade, P. S. Bernard and C. M. Perou, The molecular portraits of breast tumors are conserved across microarray platforms, *BMC Genomics*, 2006, **7**, 96, DOI: 10.1186/1471-2164-7-96.

198 L. J. van't Veer, H. Dai, M. J. van de Vijver, Y. D. He, A. A. Hart, M. Mao, H. L. Peterse, K. van der Kooy, M. J. Marton, A. T. Witteveen, G. J. Schreiber, R. M. Kerkhoven, C. Roberts, P. S. Linsley, R. Bernards and S. H. Friend, Gene expression profiling predicts clinical outcome of breast cancer, *Nature*, 2002, **415**, 530–6, DOI: 10.1038/415530a.

199 M. Buyse, S. Loi, L. van't Veer, G. Viale, M. Delorenzi, A. M. Glas, M. S. d'Assignies, J. Bergh, R. Lidereau, P. Ellis, A. Harris, J. Bogaerts, P. Therasse, A. Floore, M. Amakrane, F. Piette, E. Rutgers, C. Sotiriou, F. Cardoso and M. J. Piccart, Validation and clinical utility of a 70-gene prognostic signature for women with node-negative breast cancer, *J. Natl. Cancer Inst.*, 2006, **98**, 1183–92, DOI: 10.1093/jnci/djj329.

200 H. Y. Chuang, E. Lee, Y. T. Liu, D. Lee and T. Ideker, Network-based classification of breast cancer metastasis, *Mol. Syst. Biol.*, 2007, **3**, 140, DOI: 10.1038/msb4100180.

201 A. M. Rutman and M. D. Kuo, Radiogenomics: creating a link between molecular diagnostics and diagnostic imaging, *Eur. J. Radiol.*, 2009, **70**, 232–41, DOI: 10.1016/j.ejrad.2009.01.050.

202 E. Segal, C. B. Sirlin, C. Ooi, A. S. Adler, J. Gollub, X. Chen, B. K. Chan, G. R. Matcuk, C. T. Barry, H. Y. Chang and M. D. Kuo, Decoding global gene expression programs in liver cancer by noninvasive imaging, *Nat. Biotechnol.*, 2007, **25**, 675–80, DOI: 10.1038/nbt1306.

203 M. Diehn, C. Nardini, D. S. Wang, S. McGovern, M. Jayaraman, Y. Liang, K. Aldape, S. Cha and M. D. Kuo, Identification of noninvasive imaging surrogates for brain tumor gene-expression modules, *Proc. Natl. Acad. Sci. U. S. A.*, 2008, **105**, 5213–8, DOI: 10.1073/pnas.0801279105.